ASSAY OPTIMIZATION FOR POINT OF CARE DETECTION OF HIV

by

Aiswarya A Ramanujam

A Thesis

Submitted to the Faculty of Purdue University

In Partial Fulfillment of the Requirements for the degree of

Master of Science in Biomedical Engineering

Weldon School of Biomedical Engineering

West Lafayette, Indiana

December 2022

THE PURDUE UNIVERSITY GRADUATE SCHOOL
STATEMENT OF COMMITTEE APPROVAL

Dr. Tamara Kinzer - Ursem, Chair

Weldon School of Biomedical Engineering

Dr. Jacqueline Linnes, Co - Chair

Weldon School of Biomedical Engineering

Dr. Robert V. Stahelin

Department of Medicinal Chemistry and Molecular Pharmacology

Approved by:

Dr. Tamara Kinzer - Ursem

Dedicated to myself, my family, and friends

ACKNOWLEDGMENTS

This work would not have been possible without the support of many individuals. First and foremost, I would like to thank my advisor Dr. Tamara Kinzer - Ursem and Dr. Jacqueline Linnes for taking a chance on me three years ago and inviting me to join their lab. Under their mentorship, I have grown both professionally and personally. Their constant motivation has made me challenge myself and pursue my passions. Tami and Jackie are wonderful roles models and an incredible support system for their students. Their guidance with experimental design, analysis and don't worry attitude towards negative data has always been a strong factor in keeping my spirits up and think across the box. Their kindness and compassion have created a room for me to always go to them for any situation and not fear. I feel extremely fortunate and grateful to be under their tutelage.

I would also like to thank my thesis committee, Dr. Rob Stahelin. I met Dr. Stahelin while interviewing for my rotations and was impressed by his work. I had a chance of taking his grant writing class, and Dr. Stahelin was thorough in taking us through and patient in explaining to me the areas I needed to improve. This has honed my writing skills. Dr. Stahelin was also very understanding and kind to my decision towards switching departments and agreed to be in my committee.

The faculty and staff in the Weldon School of Biomedical Engineering are truly exceptional. Dr. Karin (Kaisa) Ejendal, is one of the best mentors I had in my research career. Her knowledge of fundamental science and her extensive skill set has been extremely helpful in troubleshooting research problems. She is also a warm and compassionate friend, who makes time for conversation about personal and professional life.

I would next like to thank Dr. Melinda Lake. I have had the pleasure of working closely with, Mindy for two years, she leads the way when it comes to bringing enthusiasm and motivation to the team, as well as connecting to people and being sensitive to one's needs. Mindy is responsible and resourceful; she takes initiative to maintain equipment and ensure that safety standards are met. She transmits her passion and talent for research to young scientists and volunteers to help students with their professional growth. I have been in awe of her time and project management skills and have been fortunate enough to learn a few.

The members of lab are extremely fun and supportive people. Navaporn (Amy) Sritong, and Emeka Nwanochie have served as a pillar of immense support throughout the last three years.

Whether it be help with experiments or a fun coffee session to destress, they are the most fun and intellectual people to work with. I would additionally like to thank Eric Tan, Jay lee, Hani Abdullah, Gunjan Saini, Hui Ma for their encouragement and collaboration over the years. I would finally like to thank my Undergraduate mentee, Winston Ngo. Winston's dedication and work ethic towards experiments, and his ability to quickly grasp and learn new skills were a huge plus and resulted in pushing experiments at a faster pace. He also provided me with an opportunity to work on my mentoring skills.

Finally, I would like to extend my gratitude to Sandra May, for her constant support and assistance in navigating through the administrative process and for always being available, when in need.

I am most grateful to my family and friends who have encouraged me throughout my educational journey and supported me with endless love and motivation.

TABLE OF CONTENTS

LIST OF TABLES

LIST OF FIGURES

LIST OF ABBREVIATIONS

Ab	Antibody
Ag	Antigen
AHI	Acute HIV infection
AIDS	Acquired immunodeficiency syndrome
ART	Anti-retro viral therapy
BLI	Bio-layer interferometry
COP	cyclic olefin polymer
HIV	Human Immunodeficiency Virus
IN	Integrase
K_3EDTA	Tri Potassium Ethylenediamine tetra acetic acid
KB	Kinetic buffer
LAMP	loop-mediated isothermal amplification
LFIA	lateral flow immunoassay
LMIC	Low - and Middle-Income Countries
LOD	limit of detection
LTR	Long terminal repeats
NAAT	Nucleic acid amplification test
PCR	polymerase chain reaction
PD	particle Diffusometry
POC	Point of care
POCT	Point-of-care testing
PWID	People who inject drugs
RDT	rapid diagnostic test
RT	Reverse transcriptase
RT-LAMP	Reverse transcription + loop-mediated isothermal amplification
TBS	Tris buffer cocktail

ABSTRACT

As of 2021, 38.4 million people worldwide are living with Human Immunodeficiency virus (HIV), with eastern and southern Africa having the highest prevalence. The efficacy of treatment is determined by identifying acute HIV infections (AHI) and prompting early antiretroviral therapy (ART) initiation to achieve viral suppression and reduce the risk of transmission. Existing rapid tests that detect host antibodies are affected by long seroconversions which allow the viruses to remain undetected until long after infection. On the contrary, highly sensitive nucleic acid amplification test (NAAT) based assays, serving as the gold standard for detection are restricted by their long turnaround time and high cost of implementation thus, restricting their use in low resource settings. Further, drug resistance cases and patient non-compliance to treatment may lead to HIV progression to aids; therefore, effective viral load monitoring is a critical component in the HIV care continuum. To address the gaps in viral load monitoring and early HIV detection, I propose to develop assays for handheld self-test platforms to detect low concentrations of HIV via two different approaches: 1) I will optimize an existing NAAT - based assay to semi-quantitatively detect HIV particles that were spiked in clinical samples and 2) I will Investigate the binding kinetics between HIV p24 antigen and Anti-HIV-1 p24 Antibody using the principle of Bio-layer Interferometry. Thus, I will lay the foundation for the development of a novel and highly sensitive p24 detection assay. Overall, this work will enable detection of ahi detection as well as support people living with HIV (PLHIV) management, all while remaining connected to healthcare and provider support.

1. INTRODUCTION

1.1 Human immunodeficiency virus (HIV) - Background and significance

HIV is a retrovirus that attacks the human immune system and breaks down the white blood cells, specifically the CD4 cells. A healthy and functioning immune system is essential to fight off infections and thereby, defend the body against diseases [1].

1.1.1 Global burden

As of 2021, 38.4 million people worldwide are living HIV, with Eastern and Southern Africa spanning the largest rate of people living with active HIV infection and Aids related death. According to UNAIDS 2022 epidemiological estimates, 650 000 people died from AIDS-related illnesses worldwide, 1.5 million people were newly infected with HIV in 2021. By the end of December 2021, of all people living with HIV, 85% knew their HIV status, 75% were accessing ART and 68% were virally suppressed. The key populations in 2021 are sex workers and their clients, gay men and other men who have sex with men, people who inject drugs, transgender people, and their sexual partners, who account for 70% infections globally. HIV falls within the genus Lentivirus, family of Retroviridae, subfamily Orthoretrovirinae, and based on the certain genetic characteristics and antigens, they are classified into two strain types, HIV-1, and HIV-2. Evolved from non-human primates in Central Africa, HIV-1 is the predominant strain responsible for the global HIV pandemic, while HIV-2 strain, from West Africa, displays reduced pathogenicity [2].

1.1.2 HIV genome and virion structure

The genome of HIV consists of 9,200-9,600 nucleotides in the case of HIV-1 and approximately 9,800 nucleotides in the case of HIV-2. Enclosed within the core of the HIV-1 genome are two identical single stranded RNA molecules. The dimeric, linear guide RNA is ~9 kb long and flanked by the 5′- and 3′- long terminal repeat (LTR) sequences. The LTR sequences code for promotor regions and contains sequences required for reverse transcription, integration, and gene expression. Group-specific antigen (*gag*) gene follows the reading frame in the 5' to 3' direction and encodes proteins p17, p7, and p24. p24 is the capsid protein is the core containing

HIV RNA, that regulates the activity of viral replication and protects the genome during the entry and exit of the virus from the host cells. DNA polymerase (*pol*) reading frame that follows gag region encodes for enzyme proteases, RNases, integrase (IN) and reverse transcriptase (RT). These enzymes carry out the mechanism of action of HIV. Next to the Pol reading frame, is the two regulatory genes rev and tat and three accessory genes *vif, vpr, and vpu*. This is followed by env reading frame, which is the outer surface of HIV that holds surface glycoprotein (*gp*) -120, and transmembrane *gp* - 40. Continuous genetic mutation and evolution has resulted in multiple subtypes, clades, and subclusters of HIV-1 and HIV-2. Based on phylogenetic analysis, HIV-1 is divided into subtype groups M, N O and P, and HIV-2 spans from groups of A-H [2]. The mature virion has a spherical shape and is enclosed by a lipid bilayer derived from the host cell. The inner layer of the membrane anchors the *gag*-derived matrix proteins (MA) and harbors *Vpr* and *PR*. The capsid is found within the center of the virion and contains the two copies of gRNA, RT, and IN. The gRNA is stabilized by the Nucleocapsid (NC*)* proteins Figure 1.1 [3].

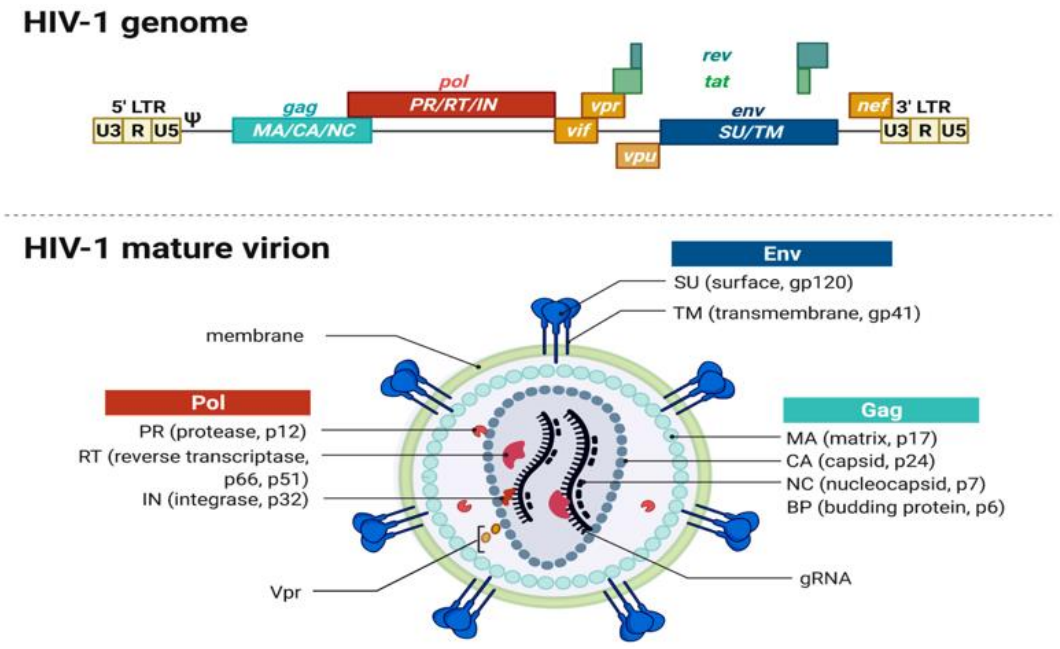

Figure 1.1. HIV-1 genome and virion structure. Top section - Schematic overview of the genomic organization of the HIV-1 RNA showing the open reading frames. Bottom section - Spherical shaped mature enveloped virion with outer Env glycoproteins and inner membrane Gag and NC proteins. Figure reprinted from "Infectious RNA: Human Immunodeficiency Virus (HIV) Biology, Therapeutic Intervention, and the Quest for a Vaccine," by Y.V Heuvel, S. Schatz, 2022, Toxins, vol. 14, no. 2, Art. No.2 [3].

1.1.3 HIV life cycle and stages of infection

Mechanism of action

HIV uses the CD4 cells to multiply and spread throughout the body. This process is carried out in seven different stages, called its life cycle. CD4 T-lymphocytes are part of white blood cells (WBCs) that organize the immune response by stimulating other immune cells, such as macrophages, B lymphocytes (B cells), and CD8 T lymphocytes (CD8 cells), to fight infection against foreign microbes [4]. The HIV mechanism of action on host CD4 cells begins by attaching itself to molecules on CD4 cells via the CD4 receptor (***step 1***). Once the binding happens, the env region of genome fuses with CD4 cell membrane. Post fusion, the virus releases its genetic material and the RT and IN enzymes (***step 2***). RT converts the HIV RNA into HIV DNA (***step 3***), and this helps the virus enter the nucleus of CD4 cell and integrate with the DNA of the host cell (***step 4***). This process of combining viral DNA into host DNA is catalyzed by the released integrase enzyme. Once, the integration occurs, HIV starts creating long chains of viral proteins using the host CD4 cells, shortly known as replication (***step 5***). The newly produced viral proteins move towards the surface of host cell and assemble into noninfectious immature HIV (***step 6***). In the last step of its life cycle, the immature HIV leaves the CD4 cell and releases the protease enzyme. This enzyme cleaves the long protein chains of the immature virus and creates the mature virus, which is capable of infecting other CD4 cells and spread further (***step 7***) [5]. This way HIV attacks the body's natural defenses gradually depleting the levels of CD4+ immune cells (T helper cells, dendritic cells, and macrophages).

If left untreated, HIV progresses to cause acquired immunodeficiency syndrome (AIDS); a condition in which the infected individual becomes vulnerable to a host of opportunistic co-infections, cancer, and other life-threatening diseases [2] [6]. Transmission of HIV is usually via body fluids from infected people during sexual contact, blood contamination in an unscreened blood transfusion or in injection drug use (IDU), and vertical transmission from mother-to-child. Everyday activities like kissing, hugging, shaking hands, or sharing personal objects, food or water however cannot infect individuals. Similarly, people undergoing antiretroviral therapy (ART) and those virally suppressed will not infect their sexual partners [6].

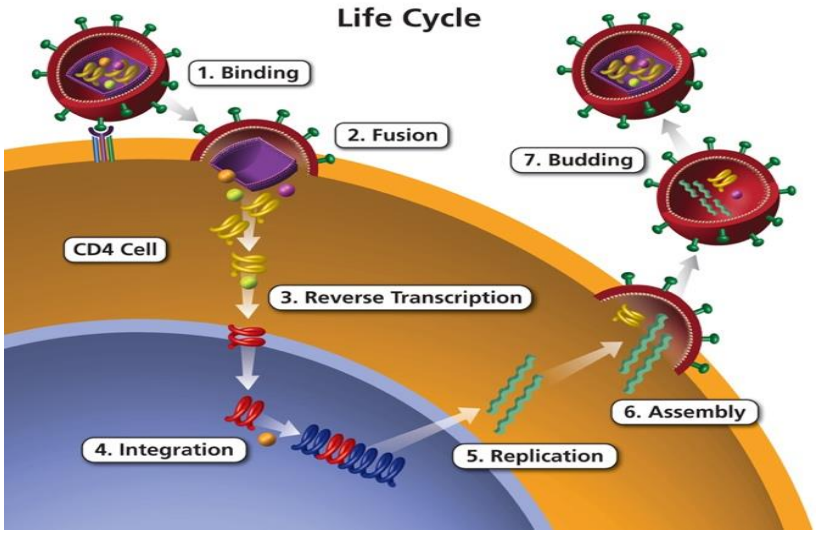

Figure 1.2- Essential steps in the HIV life cycle, figure reprinted from The HIV Life Cycle in NIH, Retrieved Nov. 01, 2022, from https://hivinfo.nih.gov/understanding-hiv/fact-sheets/hiv-life-cycle [5]

Stages of HIV infection and progression

Acute HIV Infection (AHI)

Symptoms vary from person to person, depending on the stage of disease. AHI is the first and early stage of HIV infection that develops within 2-4 weeks of infection with HIV. The infected individual presents fever, headache, rash, and other general flu like symptoms. During AHI, the virus rapidly attacks CD4 lymphocytes, replicates in number and spreads throughout the body. Due to rapid multiplication, the level of HIV in blood rises and increases the rate of transmission to other individuals. Timely diagnosis and ART during this stage can prove significant to the affected individual [7] [8].

Chronic HIV infection

This is the second stage of infection, and individuals appear asymptomatic and do not present or have any HIV related symptoms. Also, referred as clinical latency period, during this stage the virus continues to multiply inside the body in low levels. This silent stage of disease can progress quickly to AIDS in 10 years or longer if left untreated and affected population can still transmit HIV to others. Patients undergoing ART in this stage, have a chance at maintaining a low

or undetectable viral load, which also means reduced to no risk of transmitting HIV to partners through sex [8].

AIDS

AIDS is the most severe and final stage of infection. At this stage, the CD4 count is less than 200cells/mm^3 and the virus has damaged the immune system to an extent that the body cannot fight off infections. This includes the opportunistic infections that occur more frequently or show severity in immune compromised individuals. Naturally, patients diagnosed with AIDS are at high risk of transmission to others, and since the viral load is high, the survival rate is about 3 years [8].

1.1.4 Treatment

Without timely diagnosis and appropriate treatment, HIV infection can advance rapidly and worsen over time. Unfortunately, there is no available cure for HIV to-date, however, effective treatment with combination antiretroviral therapy (ART) prevents the progression to AIDS. These medicines work to suppress viral replication and improve and strengthen the weakened immune system, thereby increasing the rate of recovery and giving the affected individual a chance to fight off other co-infections. The right treatment can help people with HIV live longer and healthier lives [9]. In some cases, as soon as a patient is confirmed to be HIV positive, ART is given right away without any delay. Delaying ART initiation increases the potential for patient non-compliance and thus increases the chances of progression to AIDS in the individual. ART involves administering antiretroviral drugs and a combination of drugs from different classes to the patient to control HIV and lower the chances of viral resistance to the medications. Nevertheless, the efficacy of treatment is determined by identifying acute HIV infections or AHIs and prompting early ART initiation to achieve viral suppression and reduce the risk of transmission [10].

1.2 Point-of-care (POC) tests

Point of care testing (POCT) also known as decentralized testing involves performing a diagnostic test outside a laboratory setting to produce a rapid and reliable result that aids in identifying and managing chronic diseases and acute infections [11]. Developed in the 80s, POCT is growing in demand and has a been accepted as a rapid and economical form of diagnostic tools in comparison to conventional laboratory-based testing. They are designed to perform quantitative

or qualitative analysis of a wide range of analytes such as nucleic acids, proteins, peptides, antibodies, antigens, and metabolites [12]. The diagnostic testing industry with the USA being the world's largest single market is a multi-billion-dollar business with heavy competition and growth potential. In 2021, the market value of POC diagnostics was valued at $24.8 billion and is expected to reach $43.5 billion by 2026. This upward growth is due to the prevalence of infectious diseases. POC diagnostics, both at home testing and near patient testing helps to better manage the infectious diseases, predominantly among low income communities in developing countries with resource limitations [13].

1.2.1 Understanding the Need

Centralized laboratory testing is a critical resource model in most healthcare settings with automated high throughput laboratory instruments efficiently processing a high number of patient samples at a relatively low cost. Performed worldwide, centralized testing has remained the most dominant and relied upon model to provide results while maintaining the quality and integrity of results. Highly trained staff run in a controlled environment, perform distribution analysis, and study repeatability, and all of this is done with high automation and expensive equipment [9]. However, the model is not patient centered and does not take into consideration convenient patient access. In some cases, hospital consultation and testing are separate and require patients to complete multiple doctor visits for full clinical assessment. This imposes a problem for chronic disease patients who need to be in and out of hospitals for frequent blood tests. The inconvenience extends further for people from low socio-economic backgrounds to access large scale laboratory settings. Although, infrastructure can be made readily available for the prompt control of infectious disease in the developed world unfortunately, this is usually not the case in LMICs; tests are either unavailable or unaffordable to patients [14]. The importance of early disease diagnosis and widespread testing for the effective screening, staging, and control of infectious diseases has been re-established with the recent COVID-19 pandemic. Moreover, the pandemic in the last two years has resulted in a major decline in healthcare budget, shortage of trained personnel, material backlog. This, especially in developing countries with a growing middle class population, necessitates a need for an accessible, effective and less costly testing model that will likely bring changes to the way results are delivered in the healthcare industry [15].

POCT is needed to bring about accessible near-patient or bedside laboratory testing in resource- limited settings, provide robust results and enable prompt clinical decision making to determine a course of action or treatment for a patient [16]. Further, effective POCT can reduce a patient's length of stay, eliminate need for confirmation testing, simplify testing and operations, enable timely and proper patient isolation, reduce unnecessary downstream testing and aid with antimicrobial stewardship efforts [9].

To grow and keep up the potential of POCT in the developing world, these test kits need to meet a specific design criterion. The key requirements for an overall POC devices are that they are user friendly, storage of reagents is in a simplified, results should be concurring with established laboratory techniques, and finally is safe to use. These requirements are common for all users in all settings, however, more requirements will be depending on needs on the type of clinical setting [15]. WHO has set an ASSURED criteria for developing POC technologies to treat HIV infections, which means following these criteria the devices developed should or will be affordable, sensitive, specific, user-friendly, robust/rapid, equipment-free, and deliverable to those who need the test (ASSURED) [17]. By leveraging the high throughput functionality of dedicated centralized core facilities together with the diagnostic convenience and timeliness of POC Testing, maximum clinical diagnostic functions can be readily attained, and global health challenges can be met in resource limited settings.

1.2.2 Underlying Technology

Commercial POC and diagnostic devices available in the market have been developed with applications in glucose monitoring, pregnancy and infertility testing, infectious disease testing, cholesterol testing, and cardiac markers. Usually, microfluidics is integrated into POCT to allow for fluid manipulation and detection in a singular device with minimal sample requirements [18]. The analyte molecules being analyzed using POCT differ in their inherent chemistries such that they can each produce a unique biological signal. Therefore, the technology underlying POC is designed to isolate and transmit specific analyte signals via a built-in biosensing module comprising 3 main components: 1) biorecognition elements such as antibodies, enzymes, nucleic acids, aptamers, or molecular imprinted polymers for the selective recognition and capturing of the target analyte; 2) signal transduction mechanism for the conversion of the biorecognition signal generated by the interacting biorecognition element/analyte species, into measurable outputs

(optical or electrical), corresponding to the presence or quantity of the target analyte; and 3) display unit (computer or a printer) to aid user-interpretation of generated output signal [14], [18], [19].

1.2.3 State-of-the-Art POC Technologies

POC tests are handheld *in vitro* diagnostics designed to provide qualitative or range of quantitative measurements of biological analytical targets like proteins, nucleic acids, metabolites, drugs, human cells, etc from sample matrices like blood, saliva and other bodily fluids or (semi-)solids [16]. These devices are classified into small handheld devices or large bench-top instruments. Smaller handheld test kits are usually portable and can be used by patients without any proper healthcare training or by oral walk through by trained healthcare staff next to the patient. Some examples of smaller test kits are, at-home pregnancy test, rapid diagnostic kits (RDTs) and blood glucose sensors. The test specimen usually fingerpick or capillary sample is applied to the POC device platform, and usually the test does not require any prior labelling or need for sample container and sample transportation requirements [15]. Whereas, large bench top instruments, designed with complex built in microfluidics technology chamber are suited for outpatients. The model is like centralized lab testing, and meets sample container, labelling and transportation requirements but is differs in size and complexity which accommodate their use at the point-of care.

Paper-Based Microfluidic Platforms (Lab-on-paper)

The first functional paper-based analytical device for the parallel detection of protein and glucose analytes in urine sample were developed in 2007 by the Whiteside's Group at Harvard University [18]. Paper comprises a porous membrane network of interconnected hydrophilic cellulose fibers [20]. The spatial organization of the paper pores into 3D structures causes fluid to wick through the paper fibers by capillary pressure [21]. As a result of the inherent wicking property of paper, low-cost paper microfluidics platforms can be developed without needing expensive micropumps or power supply to move liquid reagent. Typical examples of paper based POC diagnostics, include dipsticks, urine strip tests, and lateral flow immunoassays (LFIAs) [15]. Unfortunately, paper-based platforms like LFIAs, are generally limited by their poor diagnostic accuracy, restricted to qualitative rather than quantitative analyses.

Chip-based Microfluidic Platforms (Lab-on-a-chip)

Previously, silicon and glass, inspired from the field of semi-conductors and microelectronics, were common materials for the fabrication of microfluidic chip systems. However, their application in low-cost POC devices is significantly undermined by their high material costs and fabrication complexities [21]. Polymer substrates offer less expensive and POC compatible alternatives to silicon or glass. This includes, Polyethylene Naphthalate (PEN), Polyethylene terephthalate (PET), Polyimide (PI), Polyetheretherketone, Polyethersulfone (PES),

Polycarbonate (PC), Polytetrafluoroethylene (PTFE), Cycloolefin copolymers (COC), Poly (Methylmethacrylate) (PMMA), and Polydimethylsiloxane (PDMS) [18], [21]. PDMS is largely utilized in university research-based microfluidic chip prototyping due to its biocompatibility, low fabrication cost, high optical transmittance, and gas permeability. However, PDMS usage requires special education and equipment, and currently, not many medical research centers are using this. Recent advancements in material science, modern computing, and real-time connectivity have inspired the development of next generation POC devices with improved features.

1.3 Molecular-Based Detection Assays

Molecular detection technologies greatly influence the infectious disease management and impacts prevention strategies. They have replaced the traditional testing methods and technical advancement in automation and testing models have had a critical and positive impact on treatment, care, and prompt decision-making regarding patient isolation. Molecular assays are based on nucleic acid detection of the targeted pathogen by means of (1) target amplification, (2) signal amplification, and (3) nonamplification methods.

1.3.1 Polymerase Chain Reaction (PCR)

Discovered in the 80s, Polymerase chain reaction (PCR), is the first NAAT based method and has revolutionized the field of molecular diagnostics by laying the foundation for the development of various other PCR-based techniques. PCR is used to synthesize multiple gene copies from a few copies of target nucleic acid sequence of interest to a detectable limit. The million copies or amplicons are generated by cycling repeatedly through stages of DNA

denaturation, primer annealing, and strand extension at precise temperature. Repeated thermal cycling increases the sensitivity of detection to a several hundred-fold. The reaction is run in vitro using a set of reagents like salts and buffers to support the environment for amplification, pair of target DNA specific primers (forward and reverse) to create an identical strand, and a thermostable polymerase enzyme to generate the amplicons [22]. Further, modifications were made to the basic PCR technology to increase the sensitivity and specificity of amplification. One such amplification technique is the Nested PCR - 2 primer pairs are used for amplification to bind to the original target and to the product of first pair respectively. This then amplifies a segment shorter than the original target [22].

Real-time quantitative PCR assay (qPCR)

qPCR is the current gold standard method for direct detection of pathogens from clinical specimens with superior specificity and sensitivity. A unique polymerase-fluorescent probe system is used to prime, amplify, and detect target genes [23]. Typically, a PCR assay includes the following process - (I) sample collection, (II) sample preparation - concentration or dilution of pathogens, cell membrane lysis to release genetic contents, purification, or isolation of nucleic acid from crude cultures or cell lysates, (III) amplification of nucleic acid to obtain amplicons, (IV) signal transduction, and (V) detection of the amplified product using an inbuilt florescence probe system [24]. In case of viral targets like HIV, HPV etc., Reverse-transcription PCR (RT-PCR) is employed, where in the RNA target is initially converted to its complimentary DNA (cDNA) and subsequently thermocycling is performed on the cDNA using PCR [25]. Although, qPCR demonstrates high diagnostic accuracy and throughput feasibility which allows the processing of multiple samples at a time, its widespread use is significantly hampered by the requirement for expensive laboratory equipment, sample preparation, and skilled personnel therefore, making it unfit for use at POC settings. For this reason, isothermal NAATs such as loop-mediated isothermal amplification, helicase-dependent isothermal amplification (HDA), recombinase polymerase amplification (RPA), nucleic acid sequence-based amplification, and rolling circle amplification were developed to overcome the need for temperature cycling in PCR. Isothermal nucleic acid amplification uses far less sophisticated instruments making it an attractive option for point of care applications [26].

1.3.2 Loop-Mediated Isothermal Amplification (LAMP)

Developed by Notomi et al., LAMP is a NAAT-based method that employs high strand displacing DNA polymerase and a system of four specially designed primers, two inner and two outer, to initiate auto-cycling synthesis of target gene of interest [27]. Unlike traditional PCR, the amplification of DNA copies is carried out at a constant temperature (typically 65 °C) and in less than one hour. The specificity of LAMP is linked to the recognition and hybridization of the primers to six distinct regions in the target gene. First, the inner primers (FIP and BIP) anneal with the complementary sequence within target DNA, this kicks off strand displacement synthesis. Mechanism of LAMP is shown in Figure 1.3. Further, hybridization of the outer primers (F3 and B3) to its complement releases a single stranded DNA with a looped-out structure at both ends. A stem-loop DNA is the result and that lays the foundation for LAMP auto-cycling which is mediated by the inner primers. Although, all four primers are required at early LAMP reaction stages, subsequent strand displacement and cycling steps require only the inner primers. DNA amplification is tripled at every half cycle yielding copious amounts of final LAMP products comprising stem–loop DNAs with several inverted repeats of the target and multi-looped cauliflower-like structures. These by-products may be detected either through by quantitative real time measurements of the amplicons as they are being produced or qualitative end point analysis [26] [27]. Amplicons are generated under isothermal condition by the six-region recognition of LAMP primers and a strand displacing DNA polymerase. Loop primers provide allow initiation of the hybridization of internal primers in the LAMP cycling stage to significantly reduce the total time to amplification [28] .

For detection of RNA-based target, one-pot reverse transcription (RT)- LAMP is used, where in a reverse transcriptase enzyme is added directly into the LAMP reaction mix a highly specialized variant of DNA polymerase enzyme with intrinsic reverse transcriptase activity is incorporated [26] [29]. Bacillus stearothermophilus (Bst) DNA polymerase is the strand displacing polymerase used in LAMP and increases robustness of the assay by tolerating inhibitors in the reaction [30]. LAMP is a highly sensitive, specific, and indispensable molecular tool enabling direct detection of pathogenic nucleic acids from crude samples without prior extraction steps. However, LAMP is still prone to non-specific amplification due to primer dimerization and has high sensitivity to carryover contamination [27]. Since, the LAMP assay operates at isothermal

conditions, the need for heavy thermocycler machines can be substituted with hot water baths and the single temperature feature also makes it highly suitable for POC devices [31].

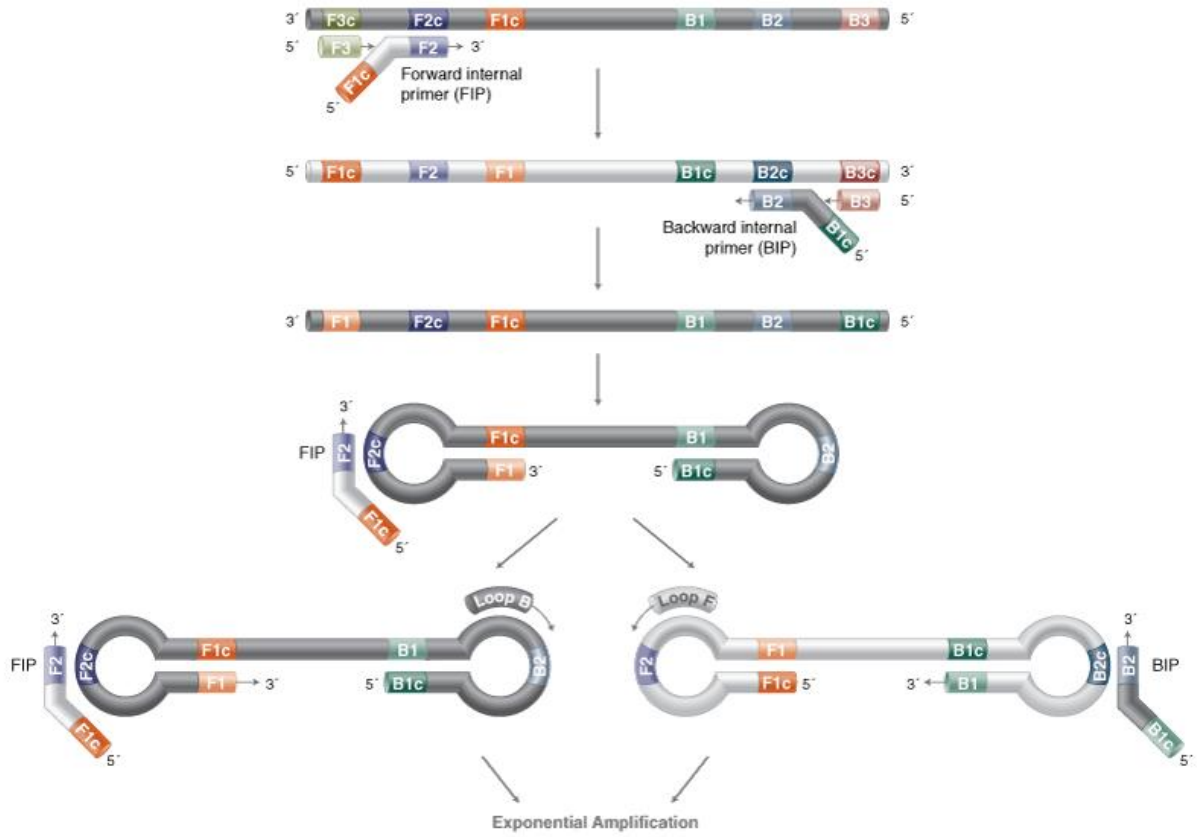

Figure 1.3-Mechanism of loop-mediated isothermal amplification (LAMP). Amplicons are generated under isothermal condition by the six-region recognition of LAMP primers and a strand displacing DNA polymerase. Figure reprinted from Loop-Mediated Isothermal Amplification in NEB, Retrieved Nov. 11, 2022, from https://www.neb.com/applications/dna-amplification-pcr-and-qpcr/isothermal-amplification/loop-mediated-isothermal-amplification-lamp. Copyrights owned or controlled by New England Biolabs, Inc (NEB). [32]

1.4 HIV Diagnostic platforms

Simplified and efficient diagnostics for HIV/AIDS without thinning the quality of patient care is a growing demand in the global health community. Low cost POC technologies like lateral flow assay and Enzyme linked immunosorbent assays (ELISA) are already well established in developing countries. Options mostly available for testing were laboratory based sophisticated platforms and as seen earlier, these require space, trained physicians, and extensive logistics when it comes to specimen care. The sooner the diagnosis, the sooner the patient can undergo ART. In other words, scaling up and decentralizing ART in resource limited communities depends upon

high quality, simple and reliable POC diagnostics [33]. Diagnostics for HIV/AIDS are usually developed keeping in mind three categories - initial diagnosis, tests to stage the patient and to monitor the patient, both before and after initiation of ART [34]. Time between HIV infection and the point when a test will give an accurate result, is the window period. A person can test negative, while having HIV and be very infectious during the window period [35]. Existing platforms for diagnosing HIV infection detect HIV antibody, HIV p24 core antigen, HIV RNA, or a combination of both anti-HIV antibody and p24 antigen. Rapid and self-tests are usually Antibody tests, and these can detect HIV 3 weeks to 3 months post exposure. A rapid antigen/antibody test done with finger prick blood can usually detect HIV 18 to 90 days after exposure. An antigen/antibody lab test using blood from a vein can usually detect HIV 18 to 45 days after exposure. A nucleic acid test (NAT) can usually detect HIV 10 to 33 days after exposure [36].

Rapid Antigen based tests

These are low cost and easy to use alternatives for sufficient decision making. Rapid tests do not require laboratory staff and can be completed in less than 30 minutes with minimal equipment. Therefore. results are obtained at the time of test and consultation [37]. Some of these include the Ora Quick Rapid HIV-1/2 Antibody (Ab) Test. Ora quick is a lateral flow rapid test that detect even low concentrations of HV antigens in oral fluid specimens. These are also available to perform blood-based tests. An alternative test available in the market, is the Aware HIV-1/2 U, relying on ELISAs and Western blots, we can obtain results with 97.2% sensitivity and 100% specificity with these tests [33].

Ag/Ab Combination tests

Combination tests like the Determine HIV-1/2 Ag/Ab Combo is an immunochromatographic rapid test that detects both antigen and antibody separately with 50% and 86% sensitivity for antigen. Rapid tests that detect the combination are especially useful for AHI diagnosis 18-90 days after exposure, since viral protein replication is here during this time, and rate of transmission and new infections also soar high during this phase [38] [39].

Antibody based tests

HIV antibodies can be detected as early as two weeks in a few people and by 12 weeks in more than 99.9% of people. An antibody test at 4 weeks will detect 95% of infections [35]. Antibody based detection assays can be performed using simple RDTs, with third generation RDTs detecting antibodies only in 60 days. Some examples of third generation RDTs are bioLytical INSTI HIV-1/HIV-2 Antibody test, MedMira Reveal G4 Rapid HIV-1 Antibody test, Chembio HIV 1/2 STAT-PAK Assay, and Chembio SURE CHECK HIV 1/2 Assay. Above listed assays use lateral flow technologies to detect HIV specific antibodies in blood, oral fluid, or urine samples [40]. However, these devices have high potential to miss AHIs because of the long period (up to 3 to 4 weeks post infection) before HIV antibody seroconversion [41]. Fourth generation Ab/Ag RDTs can detect at a window period of 45 days. Alere Determine HIV-1/2 Ag/Ab Combo and ARCHITECT HIV Ag/Ab combo are some fourth generation RDTs that combine the detection of HIV p24 antigen (appearing at about 11 days post infection) and HIV antibodies. These are able to detect the early stage infection but display low sensitivity and high implementation cost [40], [42]. Nevertheless, RDTs have to be confirmed by lab-based tests that delay the ART initiation in HIV sero positive case [42].

NAT based assays

HIV viral load characterization can be performed using non-NAT and NAT based technologies. NAT assays can detect and quantify viral RNA, and non-NAT platforms can detect and quantify HIV viral enzymes and viral proteins. This quantification will be correlated with the amount of viral RNA. NAT assays employ amplification methods like PCR, strand displacement assay (SDA), or transcription mediated assay (TMA) for detection. For HIV detection, non-NAT based assays measure the level of RT enzyme and the concentration of p24 protein and NAT based assays that look for actual virus RNA in blood, detect HIV 10 to 33 days after exposure using RT-PCR amplification strategy. Currently available RT-PCR based NATs are (i) COBAS AMPLICOR HIV- 1 MONITOR v1.5 (Roche Molecular Systems), (ii) COBAS AmpliPrep/COBAS TaqMan v2.0 (Roche Molecular Systems), (iii) Real-Time HIV-1 (Abbott), and (iv) VERSANT HIV-1 RNA 1.0 assay (kPCR) (Siemens) [16]. Since NAAT based assays, a type of NAT assays is preferred as a confirmatory test for diagnosis of early HIV infection because

they can detect HIV RNA as early as 10-12 days post infection. NAAT based assays that work by amplifying target regions in the HIV RNA genome with extreme sensitivity.

Despite the unique sensitivity of NAAT based assay in early detection, they are only used as a supplementary mode of diagnosis and their development in the field of POC NAAT platforms is slowed due to the associated complexity, high cost, and requirement for trained personnel [33] [[41]. Currently, there are only a limited number of commercially available platforms optimized for qualitative NAAT based detection of HIV near POC: Hologic Aptima HIV-1 RNA Qualitative Assay, m-PIMA HIV-1/2 Detect, Xpert HIV-1 Qualitative Assay (Cepheid), and SAMBA I and SAMBA II HIV-1 Qualitative Tests. However, Optimizing NAT based assays to operate in resource limited communities is still a challenge.

1.5 Proposed Work

By the end of December 2021, of all people living with HIV, 85% knew their HIV status, 75% were accessing ART and 68% were virally suppressed. Despite the availability and efficacy of highly active antiretroviral treatment (HAART) for HIV, this number has been a struggle to achieve. Monitoring viral load is a critical aspect to prevent the progression to AIDS. Additionally, lower viral load (< 1500 vp/ml) restricts transmission to other individuals, indicating that the HIV patient's awareness about their current viral load will help with making informed choices about their treatment as well as intimacy. Further, the risk of acquiring HIV is 35 times higher among people who inject drugs than adults who do not inject drugs [43]. People who use drugs (PWUD) are at high risk of HIV transmission and, if not diagnosed and linked to the HIV care continuum at the right time, can put even more individuals at risk and lose their chances at an improved quality of life and survival. Presently, highly sensitive NAAT based assays, which serve as the gold standard for detection are restricted due to turnaround time. Sample to answer based NAAT platforms like Cepheid's GeneXpert and Cobas LIAT HIV Quant are currently used in LMICs presently, but because of their benchtop use, they can't reach communities that are underserved by healthcare already. Existing RDTs detect host antibodies (Abs)/p24 antigen via visual readouts. Each HIV virion contains 2000-3000 copies of p24 per virus and p24 is detectable within the first months of infection prior to a host's immune response to HIV. However, in latent stages of undiagnosed HIV, the p24 antigen is complexed to the patient's own antibodies, and this is where the fourth-generation combination tests prove helpful. Unfortunately, recently FDA approved

RDTs were unable to detect HIV from a single sample in the panel spanning <102 to 5x106 vp/mL [44]. Certain other p24 based assays like Mesoscale Discovery and Quanterix detected fewer than 2x102 vp/ml but required extensive laboratory equipment for detection. Nevertheless, point-of-care nucleic acid detection assays are also limited by the exceedingly low concentration of virus in small sample volumes (1000 vp/ml is only 1 vp/μL) and it becomes increasingly difficult for assay primers and polymerase to diffuse to a single particle within a short period of time. Further, detection of RNA targets is known to have 10-100x poorer sensitivity than DNA due to inefficient reverse-transcriptase prior to amplification [45].

In addition to this, PWUD, despite being diagnosed and recognized as potential sources of transmission, are still marginalized from the mainstream HIV care continuum, due to numerous social and institutional barriers including patient and provider mistrust, high healthcare costs, and long turnaround times of current laboratory-based HIV detection [46]. To address the gaps in viral load monitoring and early HIV detection, I propose to develop assays for handheld self-test platforms to detect low concentrations of HIV via two different approaches: *1) I will Investigate the binding kinetics between HIV p24 antigen and Anti-HIV-1 p24 Antibody using the principle of Bio-layer interferometry (BLI) and 2) I will optimize an existing NAAT-based assay to semi-quantitatively detect HIV particles that were spiked in clinical samples*. The work done will be summarized here but will be explored in greater detail in Chapters 2 and 3.

Chapter 2

To achieve the first goal, **I investigated the binding kinetics of p24 Ab to p24 Ag and quantified this binding via BLI measurements using an Octet 384.** Choosing complementary antibodies binding to HIV p24 will be critical to our assay design as the binding must be efficient, specific, and rapid. Bio-Layer interferometry will provide us an evaluation of the binding affinity and rate of binding of each antibody to its target (p24). Pairs of antibodies with the most rapid p24 binding will provide the most efficient initiation of ai-LAMP assays.

Chapter 3

As part of the second aim, **I worked on optimizing the RT-LAMP assay to ensure a limit-of-detection (LOD) of HIV at <1000 vp/ml within 60 minutes.** The process of

optimization will also involve validation of assays that are predesigned and commercially obtained. To do this a) I validated the primer design for target region specificity, b) optimized assay temperature and run time, c) optimized reaction mixture composition, and d) optimized the sample matrix used in the reaction to amplify HIV. Doing this will ensure that the developed assay meets all the desirable criteria to perform efficiently under a wide range of conditions and thereby further improving our lower limit-of-detection (LLOD) and amplification resolution.

1.6 Conclusion

Successful completion of these aims will enable development of a handheld viral self-test platform to detect low concentrations of HIV. Aim 1 will allow HIV detection at quantitative level i.e., capable of determining the initial concentration of HIV RNA in a clinical blood sample. Aim 2, will provide us with kinetic measurements for HIV p24 - antibody binding and will lay the foundation for the development of a novel and highly sensitive p24 detection assay. Overall, this work will enable detection of AHI detection as well as support People Living with HIV (PLHIV) management, all while remaining connected to healthcare and provider support.

2. UNDERSTANDING THE BINDING KINETICS BETWEEN HIV P24 ANTIGEN AND ABS USING BIO-LAYER INTERFEROMETRY

2.1 Rationale

Approximately 38.4 million people living with HIV globally as of 2021. 15% of this population were not aware of their HIV status and some still needed access to testing facilities [47]. globally, 10% of new HIV infections are accounted for injection drug use. Among 11 million People who inject drugs globally, approximately 1.4 million or 1 in 8 of this population are living with HIV [48], [49]. Otherwise known as "super spreaders", the PWID population is 22 times more likely to acquire an HIV infection and also at risk of having co-infections, such as Tuberculosis (TB), and viral hepatitis B and C (HBV and HCV) [50]. Social and economic factors including patient and provider mistrust, high healthcare costs, and long turnaround times of current laboratory-based HIV detection may limit access to HIV treatment services among PWID with HIV. Immediately after HIV acquisition, the phase of transient, symptomatic illness lasts weeks to months. HIV-p24 Antigen (Ag), a structural protein that makes up most of the HIV viral core, or 'capsid' is present at very high levels in the first few weeks of infection and can be detected in the absence of anti-HIV Antibodies (Abs) [51], this is defined as the acute HIV infection (AHI). HIV concentrations in the blood rise to 10^3 HIV vp/ml within the first two weeks of infection, can spike to 10^7 vp/ml over the following months, and remain steady at an average of 10^4 vp/ml if the infection goes untreated [52]. Early detection of AHI makes patients aware of their status and allows them to link to the HIV care continuum and receive appropriate treatment for both prevention of HIV transmission and improved patient survival and quality of life Figure 2.1. The care continuum is a series of steps, that a person with HIV takes from the time of diagnosis to achieving viral suppression. However, the effectiveness of this model requires that ART treatment be initiated early in recently diagnosed individuals. Many countries do not have access to healthcare and people in low-income countries may have to go over certain barriers (financial, social, and behavioral) just to access healthcare. This is majorly how patients are lost to follow-ups, therefore, making HIV services difficult to implement.

Currently, AHI is diagnosed by detecting viral RNA in blood by nucleic acid amplification tests (NAATs) or rapid diagnostic tests (RDTs) such as the HIV capsid antigen p24 with fourth-generation immunoassays. NAATs offer high sensitivity in a range of 10–18 virions/mL, a

concentration that normally develops within two weeks of HIV infection. Paper-based RDTs are widely accessible and affordable but cannot detect AHI. Alternatively, highly sensitive molecular diagnostic assays can detect AHI, within as little as 8 days of infection, but the test requires centralized clinical laboratory settings with expensive equipment and expert laboratory technicians and is also limited to confirmation only [52].

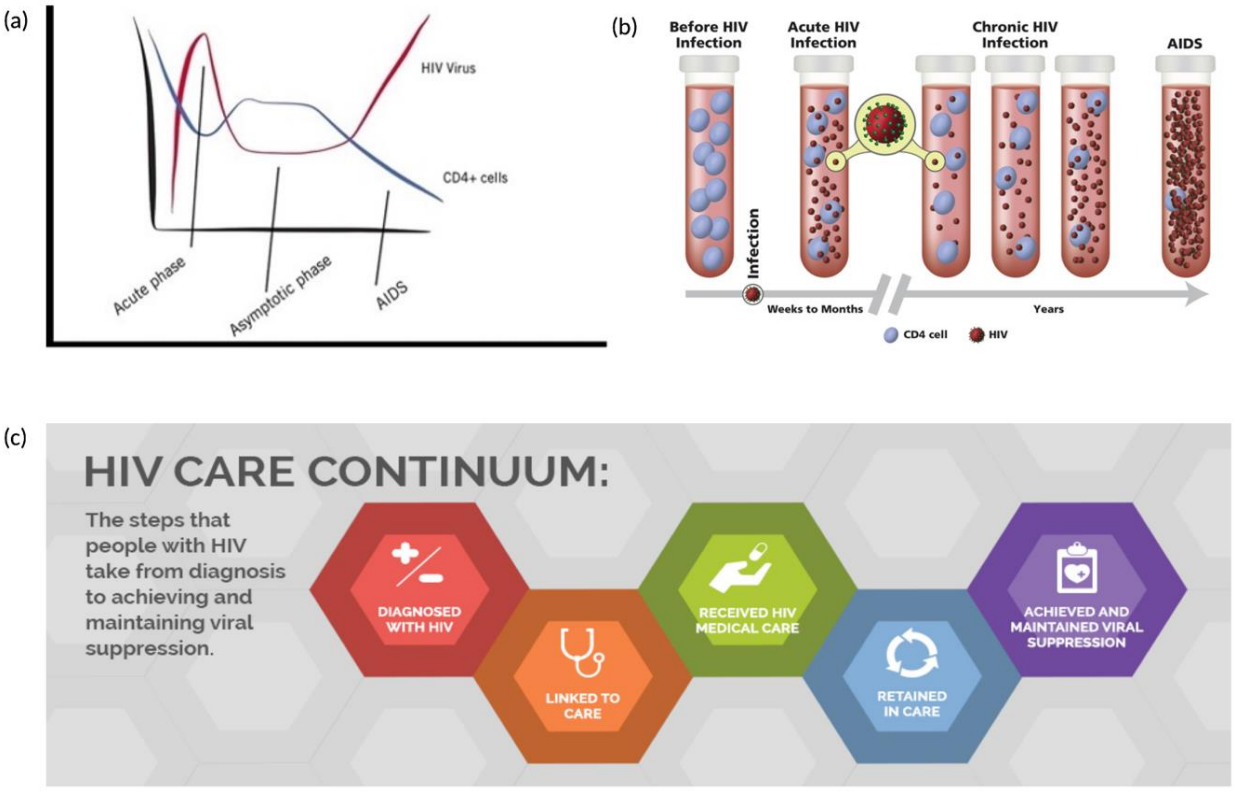

Figure 2.1- (a) Stages of untreated HIV infection, (b) HIV progression from time of infection through AIDS, (c) Model outlining HIV care continuum steps. Panel (a) is reprinted from Stages of HIV Infection in CANFAR, retrieved Aug. 08, 2016, from https://canfar.com/stages-of-hiv-infection. Copyright by Rodney Rousseau [53]. Panel (b) reprinted from The Stages of HIV Infection in NIH, from https://hivinfo.nih.gov/understanding-hiv/fact-sheets/stages-hiv-infection. Copyright by hivclinicalinfo [8]. Panel (c) reprinted from HIV Care Continuum in targethiv from https://targethiv.org/library/topics/hiv-continuum. Copyright by HIV.gov [54]

The existing gap between the testing methods platform, detection, and treatment of HIV in PWUD, warrants a need for a point-of-use (POU) approach to detect HIV in the early stage where it is most communicable to prevent transmission. The new approach will incorporate the traditional Loop-mediated isothermal amplification (LAMP) assay and develop it into an Antibody (Ab) Initiated LAMP (ai-LAMP) assay to target HIV-1-p24 Ag (like the RDTs) and generate billions of copies of target oligonucleotides detectable by the lateral flow immunoassay (LFIA). The

detection of p24 rather than RNA will account for many genetic differences in HIV-1 clades. The overall approach involves, initially labeling the Loop primers so that the positive control (standard LAMP with no Ab labeling), the Ab labeled primers, and the negative control (slower 4 primer design without loop primers) would all amplify. This will allow us to identify to what extent the Ab-Loop primers participate in LAMP. This platform for ultrasensitive POU HIV detection could transform both testing and treatment of HIV in PWUD by bringing AHI detection to substance users and care providers who are sensitive to addiction management. This new paradigm would transform the care continuum by making critical AHI detection possible at substance abuse treatment facilities, needle exchanges, and injection drug clinics. The new design must be rapid, and robust, and allow a selective detection of p24 Ag across a wide range of concentrations (1000-10^7 virions/ml) with a strong signal-to-noise ratio. Designing the ai-LAMP assay (developing a library of LAMP primer sets to target nucleic acids orthogonal to HIV and human DNA) and optimization is the first step toward this approach. These oligonucleotide target sequences will be separated into two different, complimentary strands and conjugated to different Abs [Figure 2.2].

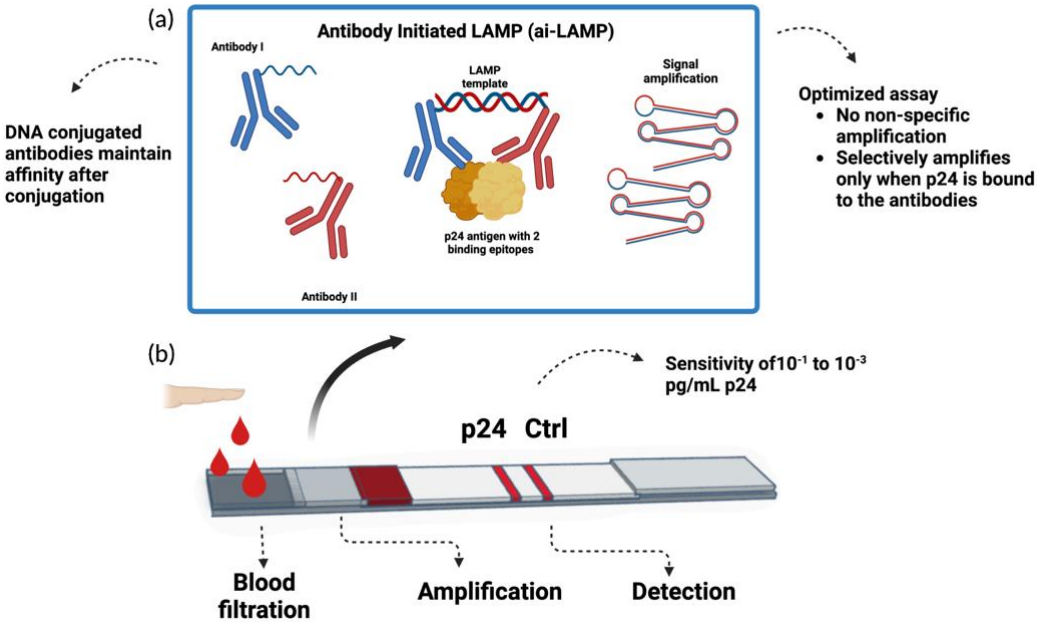

Figure 2.2. Schematic of amplification and detection. (a) Two DNA-tagged mouse α-p24 Abs bind to the p24 present in the sample and overlap to provide a template to initiate LAMP. (b) The labeled products then bind to streptavidin-conjugated gold nanoparticles and are captured by α-FITC and α-DIG Abs on the Lateral flow strip. The figures are created by Navaporn Sritong from the Linnes lab using biorender.com

The choice of complementary Abs binding to HIV p24 will be critical to our assay design as the binding must be efficient, specific, and rapid. We evaluated a library of mouse-α-p24 Abs obtained via the NIH AIDS Reagent program (Georgetown, MD) and commercial sources (e.g., Abcam in Cambridge MA, Fitzgerald Industries in Acton, MA) comparing the binding kinetics of each Ab to p24 and quantifying this binding via Bio-Layer Interferometry measurements using an Octet 384 (Forte Bio, Menlo Park, CA). Bio-Layer interferometry provides an evaluation of the binding affinity and rate of binding of each Ab to its target (p24). Pairs of Abs with the most rapid p24 binding will provide the most efficient initiation of ai-LAMP assays. The strength of interaction between an Ab and Ag is characterized by the affinity of the two biomolecules to each other; faster interaction and strong association yield a stronger complex formation. We utilized the principle of Bio-layer interferometry (BLI) using Octet RED384 optical biosensor (Forte Bio, Menlo Park, CA) to determine the binding affinity and quantify values of the association and dissociation rate constants of selected Abs to p24 Ag.

The Octet RED384 is a real-time - label-free platform that measures interference patterns caused by the binding of protein (analyte) dispensed in the sample plate to its binding partner (ligand), which is immobilized on the biosensor surface [55]. Octet system provides kinetic characterization and measures the binding between biomolecules with high sensitivity and minimal sample requirements. Dip and read biosensors used for this study are disposable after single use. A biocompatible matrix coats the tip of the biosensor, to reduce non-specific binding to the analyte in the solution. 96 or a 483 well plate is used to continuously move and measure up to 16 target biomolecules parallelly.

All Octet platforms perform based on an optical analytical technique known as BLI. This label-free technology measures the interaction between biomolecules in real time and eliminates the necessity for generating labeled biomolecules, which are time-consuming and less efficient. Thereby, BLI offers significant advantages over traditional techniques like ELISA or TR-FRET. The BLI biosensor tip has two interfaces; a biocompatible matrix to which the ligand is immobilized and an internal reference layer (optical layer). A thin layer at the optic tip separates the two layers. Light upon passing through the tip of the biosensor will reflect from the two layers separately at different wavelengths, and this forms an interference pattern. When the biosensor dips into the solution of interest, the target molecules form a molecular layer upon binding to the surface of the tip. As the number of bound molecules increases, the thickness of the molecular

layer formed increases, and this creates a shift in the interference pattern observed. This wavelength shift generated is tracked in real time and the values are plotted in a sensorgram Figure 2.3. A ligand and an analyte is used in kinetic characterization, the ligand is usually immobilized on the surface of the biosensor and the analyte is present in the solution [56] [57]. The assay begins with a baseline step – equilibrium with assay buffer, loading step - ligand is immobilized to the biosensor, Second baseline step – biosensors dipped again in assay buffer to determine the amount of ligand that has loaded on to its surface and access assay drift, Association step - immobilized biosensors dipped in the solution containing analyte and interaction between the analyte and ligand is measured, Dissociation step – the biosensor is dipped in to analyte containing solution and the bound molecules depending on their affinity or liking to the ligand will dissociate from the complex. Optimization of experimental conditions and the choice of assay buffer, biosensors, ligand, and complimentary analyte is crucial to determine the affinity and kinetic constant, as well as to obtain efficient data from the experiment [58]. The p24 Ag and the Abs selected for our experiment have a molecular weight of 28 kDa (kilodaltons) and 150 kDa respectively. Additionally, the commercially obtained p24 Ag has a polyhistidine (HIS) tag at the C-terminus, the tag is fused to enable purification and detection. Based on this, we chose the Anti-Penta-HIS (HIS1K) biosensor for kinetic analysis of p24 Ag-Ab interaction. The HIS1K biosensor, pre-coated with Penta-His Ab from Qiagen is used for capturing HIS-tagged proteins as low as 4 µL of sample from the buffer, media, or crude lysate with high affinity [59] [60]. The kinetic assay workflow is illustrated in Figure 2.4.

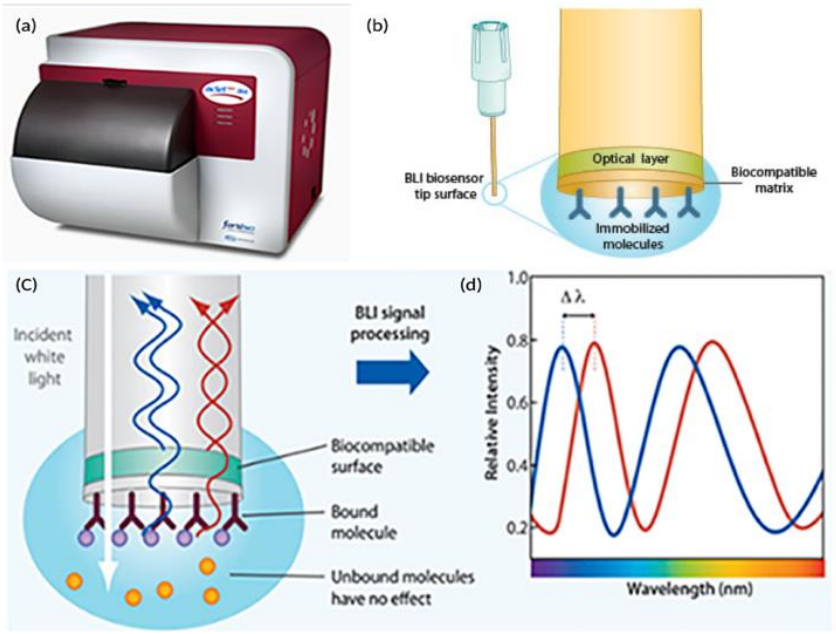

Figure 2.3- (a) - Octet RED384 instrument, (b) A Dip and Read biosensor, with the optical layer and the biocompatible layer on the surface of the tip to which ligand is immobilized, (c) Interference pattern generated upon reflection of white light from two surfaces, (d) interference pattern reported in real time. All images are reprinted from fortebio application notes, copyrighted by fortebio [61]

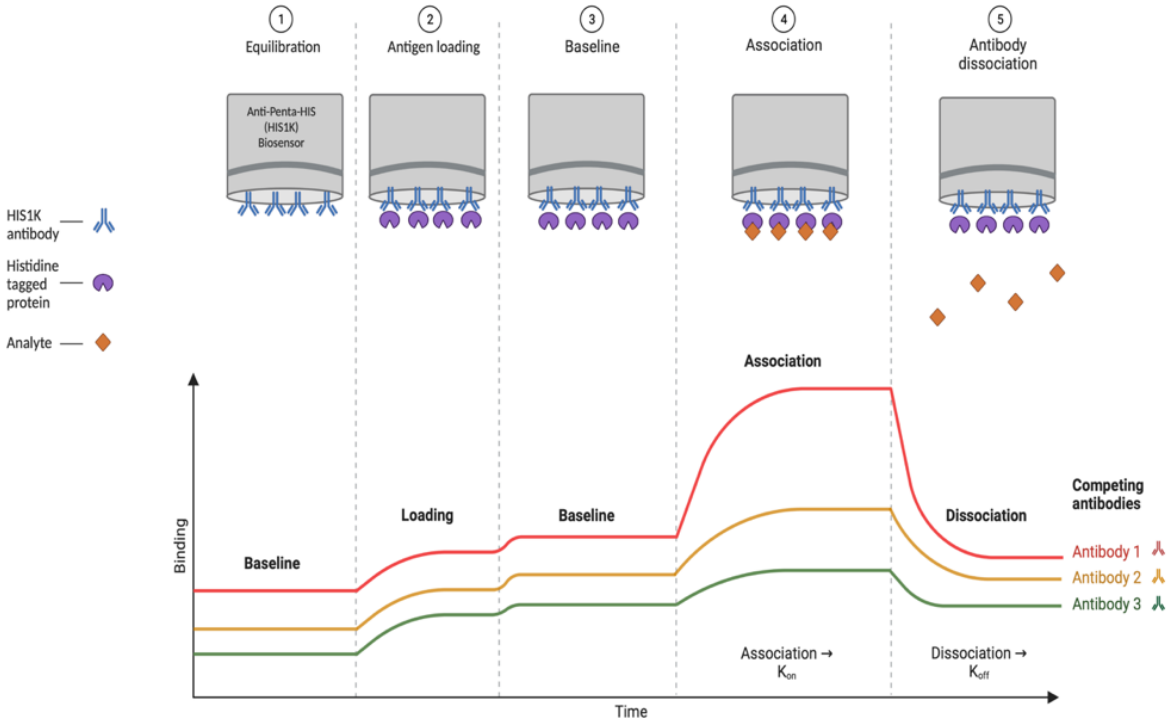

Figure 2.4- Workflow for kinetic interaction between an immobilized His-tagged ligand and an analyte using HIS1K biosensors. Figure shows the five steps in the assay - equilibration, loading of His-tagged ligand, baseline step to establish equilibrium, association, dissociation. Figure adapted and created using biorender.com

2.2 Materials

2.2.1 Antigen and Antibodies

Purified His-tagged P24 HIV-1 Ag (24 kDa) was obtained from the NIH-AIDS reagent program and HIV-1 p24 Ag protein (group M, subtype D, strain NDK) with His Tag was obtained from Sino Biological Inc. (40252-V08E). Monoclonal Abs targeting the HIV-1 p24 protein were 10-2842, 10-2843, and 10-1525 (Fitzgerald, Acton, MA), mAb246p, mAb247p, and mAb248p (BBI solutions, Portland, ME) and mAB249 and J317 (East Coast Bio, Maryland Heights, MO).

2.2.2 Kinetic binding assay reagents

Octet RED384 with data Analysis software HT 12.2 (Forte bio), Anti-Penta-HIS (HIS1K) Biosensor (Forte Bio part no. 18-5120), 96-well, black, flat bottom, polypropylene microplate (Greiner Bio-One part no. 655209), 384-well, black, flat-bottom, polypropylene microplate (Greiner Bio-One part no. 781209), Kinetics Buffer (Forte Bio part no. 18-1092), Phosphate Buffer Saline (brand, cat no.) were used for the experiments. Kinetic buffer (KB) containing the blocking agent, bovine serum albumin (BSA), and surfactant (tween-20), was chosen as the compatible assay buffer to be used throughout the assay.

2.3 Methods

2.3.1 Choice of ligand and analyte for assay orientation

The choice of the biomolecule to be used as a ligand and the analyte is very critical to the assay and depends on the size of the molecules, stability, availability of purified protein for ligand, and valency. In our case, we have 8 Abs (Molecular weight (MW)- 150KD) to be screened for interactions with the same HIS-tagged Ag protein (MW - 24KD), hence, we choose to capture the Ag protein on the surface and screen the 8 Abs. This particular ligand-analyte orientation will avoid the avidity effect or excess analyte binding to the ligand and assure a minimal dissociation drift [56].

2.3.2 Assay buffer preparation

1X KB was used for baseline stabilization as well as the sample diluent for our ligand and analyte. His-tagged P24 HIV-1 antigen was used as a ligand that is captured on the surface of the biosensor tip. To determine an optimal loading concentration, the ligand-protein was diluted with 1X KB and loaded at a concentration between 1–25 μg/ml. 1X kinetic buffer (KB) – 10-fold dilution of 10X KB with 1X PBS was performed to prepare 1X KB solution.

2.3.3 Biosensor pre-hydration

The Anti-Penta HIS1K biosensors were hydrated for at least 10 minutes before the assay with 1X KB. For the hydration step, 200 μL of 1X KB solution was pipetted into wells of a 96-well, black, flat-bottom microplate matching to the positions of biosensors. The hydration plate was inserted into the biosensor tray, and the biosensors to be used were aligned over the hydration plate by lowering them into the corresponding wells. The octet instrument was warmed up 40 minutes before the assay. The assay plate and hydration plate were placed in their respective stages inside the octet instrument for 10 minutes for them to reach equilibrium. Alternatively, sometimes a delay timer of 10 minutes/600 seconds was used to automatically start the overall binding kinetics assay. After the instrument warm-up was completed, the assay was run at 30C with a shaking speed of 1000 RPM.

2.3.4 Optimization of loading ligand concentration

For this study, we used different concentrations of p24 Ag (0 μg/ml, 2.5 μg/ml, 5 μg/ml, 10 μg/ml, 20 μg/ml, and 40 μg/ml) in duplicates to immobilize onto the HIS1K biosensor for a long step time (i.e., 15 min). Using a fixed concentration of analyte Mab 246p (16nM), an association step was performed for the different ligand concentrations mentioned above. To check for any non-specific binding of the analyte, a control biosensor with zero concentration of ligand was used. The assay was performed in a 384-well microplate in the sequence of Baseline (100 μL 1X KB), loading (100 μL of P24 antigen concentration diluted with 1X KB), baseline 2 (100 μL 1X KB), association (100 μL of 16nM mAB246p diluted with 1X KB) and dissociation (100 μL 1X KB). The initial loading response around 1.5 - 2 nm and before the saturation in the linear shape of the binding curve is considered to reduce avidity effects [61].

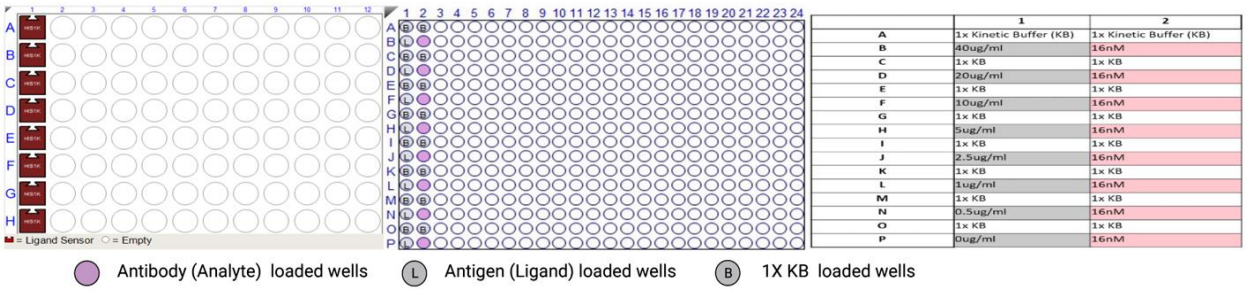

	1	2
A	1x Kinetic Buffer (KB)	1x Kinetic Buffer (KB)
B	40ug/ml	16nM
C	1x KB	1x KB
D	20ug/ml	16nM
E	1x KB	1x KB
F	10ug/ml	16nM
G	1x KB	1x KB
H	5ug/ml	16nM
I	1x KB	1x KB
J	2.5ug/ml	16nM
K	1x KB	1x KB
L	1ug/ml	16nM
M	1x KB	1x KB
N	0.5ug/ml	16nM
O	1x KB	1x KB
P	0ug/ml	16nM

Figure 2.5- Experimental setup for ligand loading optimization: (a) Sensor tray first column assigned with HIS-1-K biosensors (b) 384 sample plate layout with buffer and biomolecule in alternate wells across the column and (c) concentration map of ligand and analyte. Figure Created with biorender.com

2.3.5 Assay Parameters

All assays performed in 1X KB (prepared by diluting 10X Kinetics Buffer (Forte Bio, part no. 18-1092) 10-fold, with 1X Phosphate buffered saline (PBS, vendor, location), pH 7.4). All dilutions were carried out on the ice. A 96-well, black, flat-bottom microplate was used for the ligand-analyte binding assay and the assay was performed in duplicates in the same sequence as the loading density optimization experiment with an orbital shake speed of 1000 rpm and 10 minutes hydration time.

2.3.6 Ligand - Analyte Binding

In this assay, the Ag immobilized sensors are parallelly incubated with several different concentrations of Abs. K_{on} and K_{off} are measured, and KD is calculated from the ratees of association and dissociation. The assay is performed after validating the assay parameters and confirming that there is no non-specific binding of Ab to the biosensor in the absence of Ag.

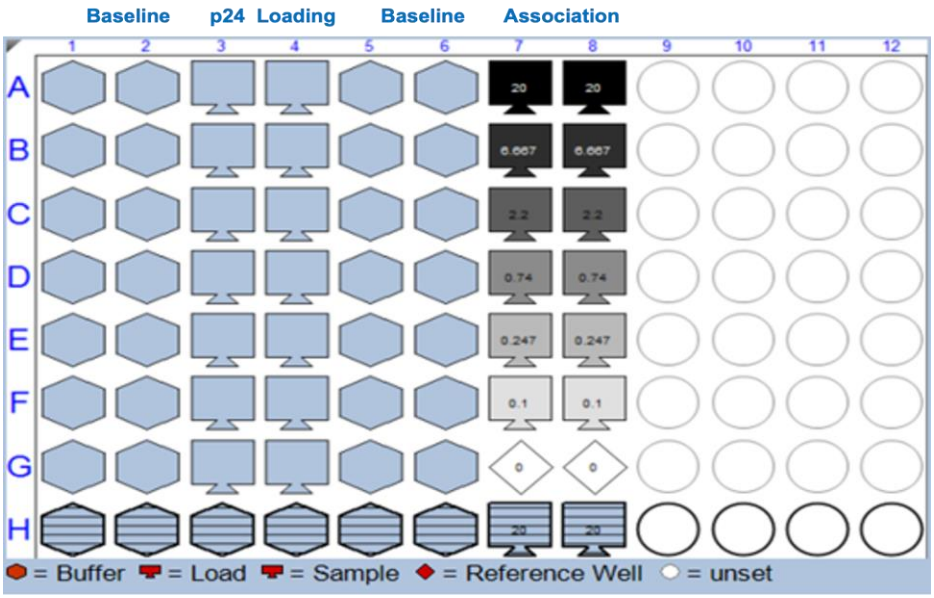

Figure 2.6- Experimental setup for determining binding kinetics between HIV-p24 Ag and complimentary Abs: 96 well sample plate layout with 1X KB, ligand and Abs loaded in 3-fold concentrations between 0nmand 20nm in wells across the column

Figure 2.7. Assay step type and run conditions

Step	Step name	Time (s)	Shake speed (rpm)	Step type
1	Baseline	120	1000	Baseline
2	Loading	160	1000	Loading
3	Wash	120	1000	Custom
4	Baseline	120	1000	Baseline
5	Association	300	1000	Association
6	Dissociation	600	1000	Dissociation

2.3.7 Binding affinity with two Abs and one Ag

this assay is performed in a tandem format where the p24 Ag is immobilized on the biosensor, followed by the saturation of the biosensor with a fixed first Ab (Ab1) and then an array of competing second Abs respectively.

2.3.8 Data processing and analysis

Upon assay completion, the raw data obtained was processed and analyzed using the Octet analysis software to determine the kinetic constants $k_{on,}$ $k_{off,}$ and the affinity constant K_D. All raw data, after the selection of specific wells and biosensors, was aligned to the baseline step. The control wells (Blank/zero concentration) sensor should not report any shift in wavelength during the assay steps. Following, the reference well subtraction, data were aligned to the association step by aligning to the y-axis. Further, inter step correction feature was used on the data to correct for any misalignment by moving the alignment to dissociation. The data was then processed by applying the Savitzky-Golay filtering to remove any high-frequency noise. The processed binding sensorgram were then analyzed by fitting the data to a 1:1 global fit curve fitting model.

2.4 Results and discussion

2.4.1 Ligand loading optimization study

In this step, the optimal antigen concentration range for adequate binding of analyte is defined and determined. We want the right amount of ligand to be loaded or immobilized to the surface of the biosensor that will offer analyte binding without introducing unnecessary artifacts in the reaction. These artifacts are an unwanted drift in the baseline, nonspecific binding to ligand or biosensor surface, and steep dissociation upon analyte binding leading to a biphasic behavior model. Loading the biosensors with a random and high concentration of ligand may introduce assay artifacts and result in analyte rebinding. The secondary binding of analyte will alter the rate constant [62].

Upon loading the HIS-1-K biosensor with several concentrations of p24 ligand and performing the association step with 16nM of mAB247p Ab, we observed that ligand concentration of 10 μg/ml of p24 Ag to immobilize to the biosensor surface resulted in optimal analyte binding response without the introduction of artifacts in the assay, and minimal baseline drift (Figure 2.7). Figure 2.7 also shows that higher concentrations of ligand (20 μg/ml and 40 μg/ml) quickly saturate the binding sites, while lower concentrations do not reach saturation. At 10 μg/mL of the ligand, we observed a significant loading signal, showing slow initial binding and a strong signal at the association step without saturating rapidly. The loading time was also calculated from the experiment, from the raw data in Figure 2.7(a), it is seen that sensor loaded

with 10 µg/ml of Ag (light blue, third curve) attains saturation at about 160 seconds from the time of loading (taking in mind that the baseline stabilization time is subtracted from overall loading time). So, we use a constant 160 seconds of loading time for all experiments going forward.

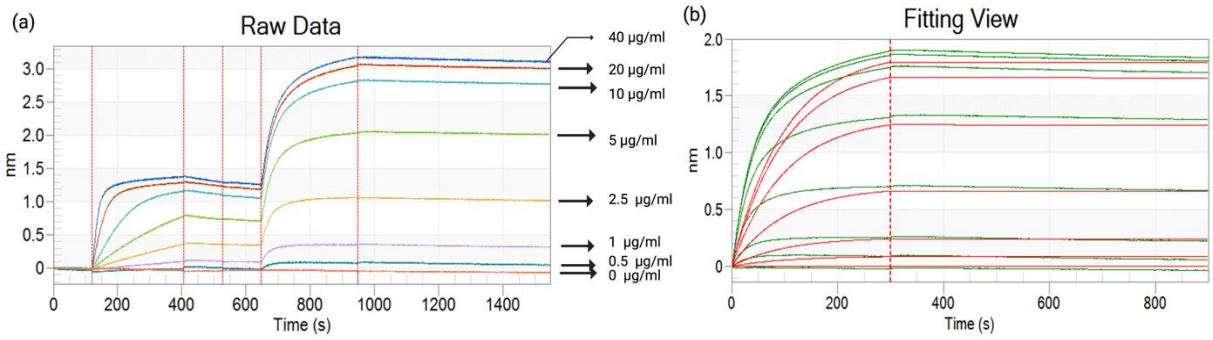

Figure 2.8- (a) Raw data for ligand loading optimization experiment showing the interaction between several concentrations of ligand His-tagged P24 HIV-1 Ag (24 kDa) and single concentration of analyte mAb246p (150 kDa) using Anti-Penta-HIS1K biosensor on octet 384. (b) Fitting view sensorgram traces showing association and dissociation steps and a good alignment with hypothetical binding curves (curve fit lines in red). When the data is fitted, we can observe the difference in analyte signal upon binding with each ligand concentration (c) Kinetic analysis results show KD value in the Picomolar (pM) range indicating a tight binding between the biomolecules. Figure created with biorender.com

2.4.2 Kinetic characterization of antibody-antigen interaction

A kinetic reaction measures how quickly a molecule binds to another molecule (association) and how quickly it falls apart (dissociation). An equilibrium is established once the complex is formed and after that point, the rate of association and rate of dissociation is the same, and so is the unbound molecules and bound molecules ratio. The strength of bound molecules once after they reach the equilibrium is referred to as the affinity. The equation below represents the interaction between two biomolecules:

$$A + B \leftrightharpoons AB$$

where *A* indicates the molecule that will be immobilized on the surface of the biosensor, and *B* is the target biomolecule in solution. The equation follows pseudo-first-order kinetics. The rate of complex formation (*AB*) is based on the association rate constant, $k_{on,}$ and the concentrations of unbound ligand and analyte. k_{on} or k_a, expressed in $M^{-1}sec^{-1}$, represents the number of AB complexes formed in 1 molar solution of A and B every second. The dissociation rate constant,

k_{off} or $k_{d,}$ represents the stability of the complex, or the fraction of complexes that decay per second, and is expressed in units of sec^{-1}. The affinity constant, K_D is derived from this equation and is expressed in molar units (M).

$$\boxed{K_D} = \frac{[A].[B]}{[AB]} = \frac{k_{off}}{k_{on}}$$

K_D is the concentration of analyte at which 50% of ligand binding sites are occupied at equilibrium or the concentration at which the number of bound and unbound molecules are the same. Affinity and K_D are related inversely, i.e., the smaller the K_D value, the tighter the interaction between the molecules, and the greater the affinity. Similarly, if the dissociation is faster, then the K_D value is larger. When the association phase reaches the equilibrium binding signal (Req), the binding curve flattens. This binding signal reaches a maximum when the maximum amount of analyte is bound to the ligand, given by R_{max}. Using the raw data, fitted data from the processed values, and rate constants computed from the data can provide us information on the quality of fit.

As already seen above, a kinetic assay of two biomolecules involves one or more baseline steps, a custom wash step if needed, an association step, and a dissociation step. It is important to establish the baseline before association to minimize the drift. Baseline drift also impacts maximum binding capacity, or R_{max} [63]. We perform baseline stabilization by dipping the biosensors in the same kinetic buffer solution used throughout the reaction for dilutions. It is important to not change the buffer solutions used in binding characterization as it might results in interference of buffer composition with the reaction. Using the established assay conditions such as assay run time, shaking speed, and optimal ligand loading concentrations were experimented to observe the strength of interaction between ligand His-tagged P24 HIV-1 Ag (24 kDa) and several concentrations of analyte mAb246p (150 kDa) using HIS-1-K biosensor. The two control (Blank) sensors, which are incubated with zero ligand and only antibody, and Free analyte and Ag do not display any wavelength shift during the association and dissociation steps. Thus, providing us with accurate measurements for Ab affinity towards its ligand. It is crucial to validate that the antibody dissociates at a rate faster than its dissociation from the biosensor. From the binding sensorgram results, we observed a tight binding of biomolecules

while testing 3-fold serial dilution concentrations of all 8 analytes with p24 Ag in duplicates. The K_D values were found in the picomolar range and the R^2 value above 0.95 was obtained for all Ag- Ab pairs. Although, the uneven spacing between the association curves indicates that the ligand binding sites might have been saturated by a high concentration of analyte, increasing the potential for some non-ideal behavior related to non-specific binding or aggregation. This does not affect the results as much since our binding curve shows a 1:1 binding interaction with a monophasic binding curve and a good agreement with hypothetical binding curves in red. Global fit was used for fitting the analyzed data between range of analyte concentrations using same rate constants. This would offer a robust and exact estimation of binding between molecules [63].

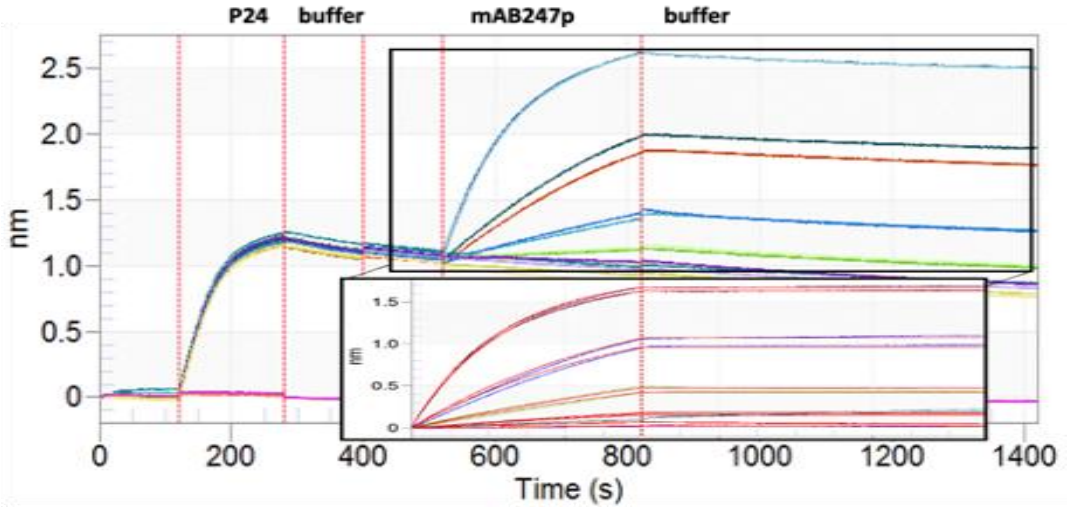

Figure 2.9- Interaction between ligand His-tagged P24 HIV-1 Ag (24 kda) and analyte mab247p (150 kda) using HIS-1-K biosensor. Assay was performed at 30°C using 1X Kinetics Buffer. 1:1 binding used to process the data and provide a curve fit. Fitting view is shown right below the real time view in the figure

Figure 2.10- KD value, kon and koff rates for interaction between ligand His-tagged P24 HIV-1 Ag (24 kDa) and analyte mAb247p (150 kDa) using Anti-Penta-HIS biosensor

p24 - mAB247p	KD (M)	kon(1/Ms)	koff(1/s)
Average	1.20E-10	1.75E+06	3.44E-04
St. dev.	9.96E-11	2.90E+06	3.91E-04

2.4.3 Kinetic characterization of a pair of antibody-antigen interactions -

The tandem format assay represents the degree of competition between a pair of Abs and the Ag. After testing the binding affinity of four different Ab pairs and the p24 Ag, mAB247P, which was used as Ab1 saturates with a flat line and does not dissociate quickly indicating that it is still bound to Ag. The KD value looks promising in the range showing a high affinity, confirming the previous results for interaction between p24 Ag-mAB247P. The association rate of binding Ab2 in each pair with Ag produces a shift in the wavelength pattern indicating that Ab2 is not competing for the same epitope as Ab1 and does not interfere with the binding to the same Ag. Additionally, the dissociation curves do not fall rapidly, and the curve fit data shows reliable fitting with the hypothetical curves in red, and finally, KD values for all Ab2s are in the low nanomolar range, which shows a strong affinity for the interaction.

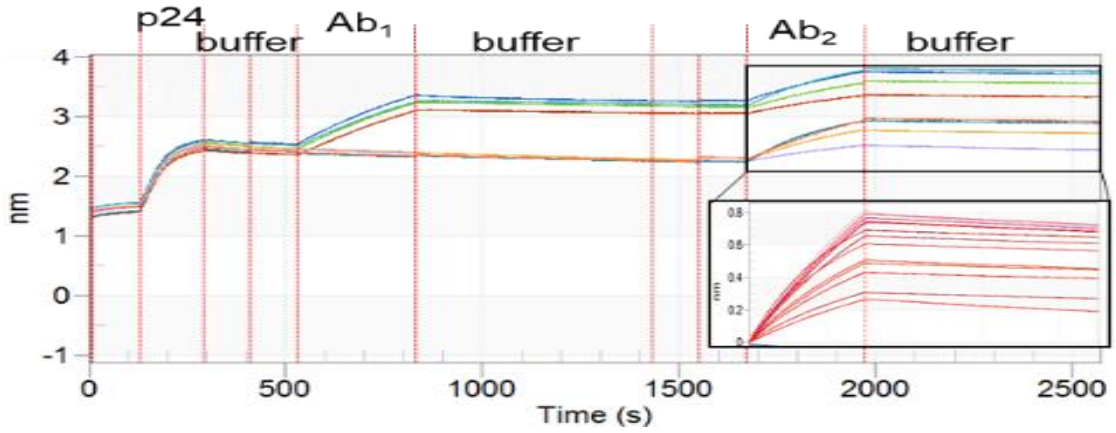

Figure 2.11. Interaction between ligand His-tagged P24 HIV-1 Ag (24 kda) and a pair of analytes (150 kda) using HIS-1-K biosensor. Assay was performed at 30°C using 1X Kinetics Buffer. 1:1 binding used to process the data and provide a curve fit. Fitting view is shown right below the real time view in the figure.

Figure 2.12. KD value, k_{on} *and* k_{off} rates for interaction between ligand His-tagged P24 HIV-1 Ag (24 kDa) and pair of antibodies (150 kDa) using Anti-Penta-HIS biosensor.

p24 Ab pair	KD	Kon	Kof
247-246	6.80E-10	2.20E+05	1.50E-04
	4.30E-10	3.40E+05	1.50E-05
247-248	6.80E-10	2.20E+05	1.50E-04
	5.10E-10	4.10E+05	2.10E-04
247-249	6.80E-10	2.20E+05	1.50E-04
	2.10E-10	5.60E+05	1.20E-04
247-J317	6.80E-10	2.20E+05	1.50E-04
	3.80E-10	3.80E +05	1.50E-04
Average	5.30E-10	3.20E+05	1.40E-04
St. Dev.	1.80E-10	1.30E+05	5.50E-05

2.5 Conclusion and future directions

The selection of complementary antibodies binding to HIV p24 will be important to the design of our assay. The binding between antibodies and p24 antigen must be specific and fast to yield a strong antigen-antibody complex. We have evaluated the binding affinity of mouse-α-p24 Abs to p24 Ag by comparing the binding kinetics of each Ab to p24 and further quantifying this binding via Bio-Layer Interferometry measurements using an Octet 384 (ForteBio, Menlo Park, CA). Based on the results from kinetic characterization via both tandem assay as well as single Ab-Ag interaction, we have picked mAB246p, mAB247p, and mAB248p (BBI solution, Cardiff, United Kingdom) as most efficient initiation of ai-LAMP assays.

Moving forward we will conjugate the chosen mAbs with the partial oligonucleotide sequences to form Ab-DNA probes. We will then optimize the ai-LAMP design to detect HIV p24, by titrating in varying concentrations of Ab-DNA strands, primers, and p24. The results will be confirmed with endpoint gel electrophoresis and LFIA. The robustness of the optimized ai-LAMP assay will be assessed by titrating in concentrations ranging from 0-30% plasma and whole blood following ISO standards. The efficiency of LFIA and its response to off-target compounds will be tested by adding a high concentration of Human DNA, proteins, nucleic acids, non-HIV viruses, and bacterial pathogens into the assay.

Overall, by pairing the sensitivity of LAMP and the selectivity of p24 antibodies, we will develop an ultrasensitive platform to detect HIV p24 from whole blood with a visual LFIA readout. Capable of detecting low concentrations of HIV (<1000 viral copies/ml) and covering the viral load threshold requirements, this simple yes/no HIV self-test will be applied for both AHI and chronic HIV infection. Overall, this sample-to-result molecular diagnostic test will address the critical gap within the existing HIV diagnosis and care continuum linkage among PWUD.

3. OPTIMIZATION AND VALIDATION OF HIV RT-LAMP ASSAY

3.1 Scientific Premise

For people living with HIV, routine viral load tests improve treatment quality and individual health outcomes. Viral load testing contributes to prevention, and potentially reduces resource needs for costly second- and third-line HIV medicines. In addition to the above, viral load testing is an essential component to ensuring an effective antiretroviral therapy (ART) and motivating patients to continue treatment, thereby minimizing likelihood of HIV accumulating drug-resistance mutations. A viral load test measures the number of HIV viral particles (vp) per milliliter of blood. A low viral load indicates that treatment is effective. A high viral load in a person on treatment indicates either that the medication is not being taken properly or that the virus is becoming resistant to the medication [64]. The UNAIDS 95-95-95 goals, re-strategized in the end of 2020, called for 95% of the HIV infected population being made aware of their status, 95% of those who knew their status be linked to antiretroviral treatment, and 95% of those being treated obtaining sustained viral suppression. Previously, framed 90-90-90 targets was not met globally and reaching the current 95-95-95 goals require doubled efforts, to avoid HIV related deaths and increased infections due to delayed public health response [65]. As of 2021, 85% knew their HIV status, 75% were accessing ART, and 68% were virally suppressed [47]. An effective ART is to achieve a viral suppression so low that the viral load cannot be detected by viral load testing. The most accurate way of determining whether the ART is successful in suppressing the viral replication is to perform periodic viral load testing [64]. The greatest challenge in achieving the UNAIDS goal, is engaging the diagnosed population in medical care to achieve viral suppression. Patient non-compliance in the form of behavior, access to timely and proper healthcare and the socio-economic barriers play an important role as to why people might not come forward towards treatment.

3.1.1 Rational

Concentrations of HIV RNA in whole blood rise to detectable levels within the first two weeks of infection and if left untreated, the concentrations remain steady corresponding to an average of 10^4vp/ml. Due to rapid and continuous rise in RNA levels during early infection and

rapid reduction in response to treatment, measurements of HIV RNA concentrations in blood is the gold standard for laboratory-based diagnosis and viral load monitoring [66]. Routinely used tests for HIV diagnosis detect the HIV p24 antigen and patient generated HIV antibodies. However, because antibodies are completely unresponsive to treatment failure and quantification of p24 is unreliable at HIV viral load concentrations below 10^4 vp/ml, these tests are not performed for routine viral load monitoring [66],[67]. On the contrary, highly sensitive Nucleic Acid Amplification Test (NAAT) based assays, serving as the gold standard for detection are restricted by their long turnaround time and high cost of implementation thus, restricting their use in low resource settings. Further, drug resistance cases and patient non-compliance to treatment may lead to HIV progression to aids; therefore, effective viral load monitoring is a critical component to reach those who are currently lost in follow up or those not engaged in routine testing and in their linkage to HIV care continuum. By developing an easy-to-use, reliable, and highly sensitive self-test platform, we can aim at reducing patient non-compliance and achieve an increased viral suppression by enabling patients to monitor their own viral load within the convenience and privacy of their own homes. Proposed handheld HIV viral load self-test is being designed to empower people living with HIV to monitor their HIV health status and will help reach the worldwide UNAIDS 95-95-95 goals. The device will be a smartphone-based sample to answer platform that is able to quantify HIV from a finger prick blood sample by applying Particle Diffusometry (PD) and Reverse Transcription Loop Mediated Isothermal Amplification (RT-LAMP).

3.1.2 Particle Diffusometry

PD is an analytical technique that measures the diffusivity or diffusion coefficient (D) of particles suspended in solution as a function of the temperature (T), solution viscosity (η), and the radius of the particle (r) in solution according to the Stokes-Einstein equation [68]:

$$D = \frac{kBT}{6\pi\eta r}$$

PD estimates the diffusion coefficient of particles by imaging the Brownian motion of the particles in a liquid and detecting the changes in the physical properties of the solution. We have performed a 60-minute LAMP assay using a biotinylated Loop-F primer and added 400 nm streptavidin-

coated fluorescent nanoparticles to induce a change in particle size that alters PD measurements along with changes in solution viscosity. This combination of PD and RT-LAMP will separate HIV virions from its associated DNA/RNA, lyse the virions, and amplify the target sequences of the virion. The amplification will increase the particle size of virions as well as the viscosity of solution, and then these particles can be detected and quantified by the smartphone-based measurements. This technique has been proven effective in the amplification of V. cholerae ctxA gene with biotinylated loop primers [69]. Figure 3.1 describes the working mechanism of Nucleic acid amplification and PD in detection and quantification of virions.

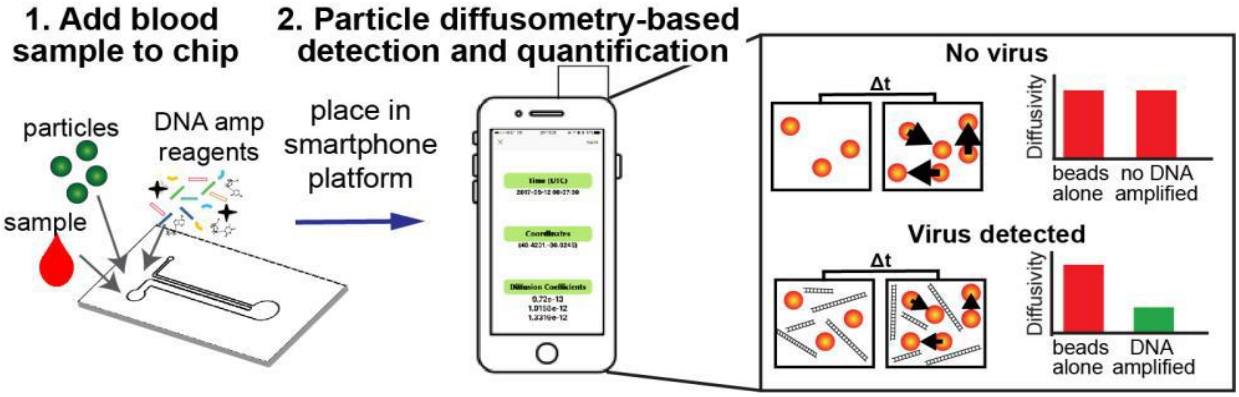

Figure 3.1: 1) Blood from a finger prick is loaded into a microfluidic chip that contains particles, enzymes, and oligonucleotides for RNA amplification via RT-LAMP. 2)The chip is placed into the hardware platform, and viral RNA is amplified. Images of particle motion are analyzed. Decreases in particle diffusivity are used to calculate the number of virions in a sample. Image credits - Dr. Linnes

3.1.3 Research Approach

To develop the proposed device, assay development and optimization is an essential criterion. The process of optimization will also involve validation of assays that are predesigned and commercially obtained. Doing this will ensure that the developed assay meets all the desirable criteria to perform efficiently under a wide range of conditions and thereby further improving our lower limit-of-detection (LLOD) and amplification resolution. Below I will detail our efforts in optimizing the currently used isothermal nucleic acid amplification assay, to detect $<10^3$ HIV vp/mL within 60 minutes and ensure that it differentiates between invalid tests and undetectable HIV viral load. To achieve this a) I validated the primer design for target region specificity, b)

optimized assay temperature and run time, c) optimized reaction mixture composition, and d) optimized the sample matrix used in the reaction to amplify HIV.

3.2 Materials and Methods

3.2.1 Viral Target

HIV viral particles (HIV-1 RNA AccuSpan Linearity Panel 2410-0221, Sera care Accuspan) were serially diluted 10-fold with non-DEPC treated nuclease free water (Invitrogen, Carlsbad, CA). Isothermal incubation at 65°C was performed for 60 min in a QuantStudio 5 Real-Time PCR machine (ThermoFisher, Waltham, MA). Obtained from serial dilutions of a cultured virus with established reactivity for HIV-1 (Human Immunodeficiency Virus 1), these whole viral particles are made replication deficient HIV-1 strain by making a point mutation within the genome of the virus due to their cultivation in 8E5 clonal cell line.

3.2.2 Sample Matrix

Whole blood with Sodium Citrate (Innovative research, Novi, MI) and Whole blood with Tripotassium Ethylenediaminetetraacetic Acid (K_3EDTA) (BioIVT, USA) was used as the sample matrix at up to 5% (v/v) of the final reaction volume for experiments. Centrifuging whole blood results in separation of red blood cells (RBCs), plasma and platelets. Heavier cells like RBCs sink at the bottom, giving a yellow supernatant called plasma which is 55% of blood [70]. The choice of anti-coagulant is very important in molecular assays that employ whole blood, as it could interfere with the results or in some cases inhibit the process. The whole blood we use is collected in K_3EDTA anticoagulant. EDTA does not distort blood cells and inhibits the clotting of blood by removing or chelating calcium from whole blood. EDTA is also an excellent chelating agent and binds with any cations Ca^{2+}, Mg^{2+} in a 1:1 manner regardless of the charge in the cation, thus effectively reducing the concentration of Mg^{2+} or Ca^{2+} in any reaction. Magnesium in the form of $MgCl^{2+}$ in the master mix has a significant impact on the efficiency and specificity of PCR reactions, the cation influences the polymerase activity and increases amplification. To combat this effect of interaction between EDTA and Mg^{2+}, the concentration of Mg^{2+} is increased in the reaction mixture that will compensate for bound Mg^{2+} [70].

3.2.3 Reverse transcription loop mediated isothermal amplification (RT-LAMP)

RT-LAMP was performed using primers designed to target the HIV-HXB2 gene of HIV-1 subtypes (Table). The LAMP reaction mixture (25 μL) contained the following components (list table): 1.6 μM FIP/BIP primers, 0.2 μM F3/B3 primers, 0.4 μM LF/LB primers (Integrated DNA Technologies, Inc.), 2X Warmstart RT-LAMP master mix (New England Biolabs, Ipswich, MA), 200 μM dUTP (New England Biolabs, Ipswich, MA), 1X UDG (New England Biolabs, Ipswich, MA), 1x ROX Reference dye (Invitrogen, Carlsbad, CA), 0.2x Eva Green (Fisher, Hampton, NH), 0.2mM $MgSO_4$ (Invitrogen, Carlsbad, CA) with 4 μL of template (5% centrifuged blood and plasma)experiments in a total volume of 25 μL. For all preliminary, in-tube amplification experiments 400 nm streptavidin coated Dragon Green fluorescent particles (Bangs Laboratories, Inc. Fishers, IN) were added to the reactions at a final concentration of prior to amplification. For on-chip experiments tested later using in-house fabricated microchips (List appendix), the fluorescent beads were added at the same final concentration. RT-LAMP products were visualized using an ethidium bromide stained 2% agarose gel at 100V for 50 min. The gel was imaged using an ultraviolet light gel system (c400, Azure Biosystems, Dublin, CA). Gel images were collected using Azure Series software at settings of UV302 after a 15 second exposure. The amplicons were stored at 4°C until analyzed with the smartphone-based PD platform [71].

3.2.4 Statistical Analysis

All PD measurements to determine statistical significance of HIV-RT-LAMP products were compared to negative controls (NTC) with a one-way ANOVA post-hoc Dunnett's test. To compare every positive control to every NTC, Tukey's multiple comparison test was used. Box and whisker plots were generated for the PD data where the upper and lower bounds of the boxes represent the 75th and 25th percentile about the mean, respectively, and the minimum and maximum values are represented by the upper and lower whiskers [71].

3.3 HIV RT-LAMP Assay Optimization

3.3.1 Primer re-design

Human immunodeficiency virus type-1 (HIV-1) is an enveloped virus that encodes two envelope (Env) glycoproteins - the surface (SU) glycoprotein gp120 and the transmembrane (TM) glycoprotein gp41, four major *gag* proteins—matrix (MA), capsid (CA), nucleocapsid (*NC*), and p6—and the *pol*-encoded enzymes protease (PR), reverse transcriptase (*RT*), and integrase (*IN*) [72]. The *gag* proteins are polypeptides that can form virus like particles in-vitro in the absence of viral and cellular components. The *gag* proteins assemble in the plasma membrane and play a crucial role in HIV-1 virus particle assembly, release, and maturation. IN is an essential viral enzyme, comprising 288 amino acids encoded by the 3′-end of the HIV polymerase gene. HIV-1 uses integrase to insert its viral DNA into the DNA of the host CD4 cell. Integration is a crucial step in the HIV life cycle and is blocked by a class of antiretroviral (ARV) HIV drugs called integrase strand transfer inhibitors (INSTIs) [73] [74].The majority of antiviral drugs target RT and PR enzymes making *gag* gene less prone to genetic mutation, and since HIV-1 will try to conserve the IN gene as much as possible to keep the chromosomal integration into host intact, makes them potential targets in our assay.

Former lab members designed two RT-LAMP assays in blood plasma that detects HIV-1 *gag* gene and *integrase* gene across the major HIV-1 Group M subtypes to provide increased clinical sensitivity. However, the assay was prone to non-specific amplification and the LOD was only 10^4 vp/rxn. To minimize this and improve sensitivity, the existing primers were redesigned by identifying and correcting the nucleotide mismatches in the original design using in silico primer analysis tool (Primer Explorer V5). The LAMP assay as discussed earlier, makes use of 4-6 primers recognizing 6-8 distinct regions of target DNA. We input 6 main primers in our assay: F3, B3, FIP, BIP LF-bio, & LB. Each set contains four primers, FIP (Forward Inner Primer - F1c-F2), F3, BIP (Backward Inner Primer- B1c-B2) and B3, and additional loop primers LF and LB. F1, F2, F3 are usually about 20bp long sequences selected from the target gene. B1, B2, B3 are also about 20bp long sequences selected from the complementary strand. F1c and F1, B1 and B1c are complementary regions. In a valid orientation, the B1 and F1 primers are aligned in the center and the B2 and F2 primers are aligned outside them Figure 3.2. If the mapping to the target input

is ambiguous or the primers do not align to the target in an acceptable orientation the results will not be generated [75] [27].

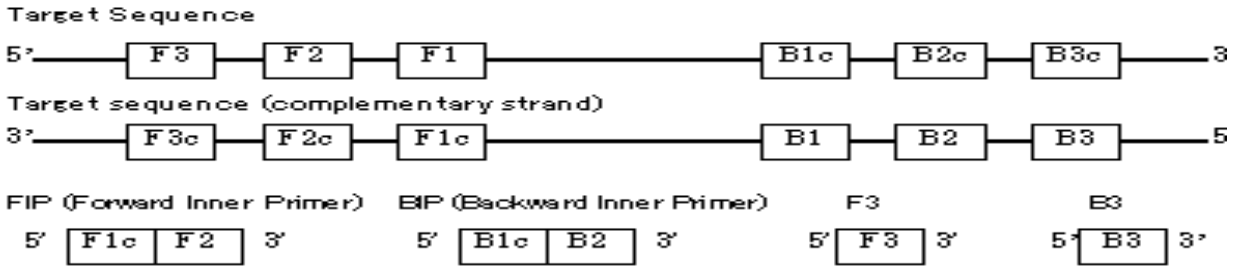

Figure 3.2. Location and orientation of primers in a LAMP assay

After checking for sequence alignment and orientation errors by comparing to recommended primer designs and by restriction analysis of integrase (base 4700-4950). There was an overlap found between F3 and F2, for which a point deletion in F2 was performed by moving F2 one nucleotide position to the right until the 3' end meets "G". Integrase primer optimization by Emeka Nwanochie, graduate student, TKU lab.

The *gag* primers detected the HIV-1 gag gene from HIV-1 HXB2 (a clone of HIV-1 IIIB isolate). After a sequence alignment check across the P17 region of gene covering flanked by base pairs 852-1052, no nucleotide addition, deletion or overlap found in the designed primers. Therefore, a spacer sequence containing 4 Thymine nucleotides (TTTT) was introduced between FIP and BIP, i.e., between F1c & F2 and B1c & B2, to provide more flexibility and improve analysis.

The performance of the newly designed HIV-1 integrase gene primer set, and *gag* gene primer set was further evaluated in a RT-LAMP reaction setup using contrived plasma samples obtained by centrifuging whole blood at 2000 rpm for 10 minutes at room temperature.

The reaction with the *gag* primer set, using Bst 3.0, a New England Biolabs product that combines the RT and polymerase), was performed at 65°C and achieves amplification from as few as 10^1 copies of purified HIV-1 virus/reaction.

3.3.2 Effect of different BST polymerases and enzymes

We investigated effectiveness of different DNA polymerases in improving the efficiency of our assay. Bst DNA Polymerase is an enzyme derived from the large fragment of Bacillus stearothermophilus DNA Polymerase I. It contains 5´- 3´ DNA polymerase activity and strong strand displacement activity but lacks 5´- 3´ exonuclease activity. The polymerase is optimized for isothermal amplification, ideally proving rapid and specific for LAMP assays at a constant temperature of 60-65 °C [76]. Bst 3.0 is engineered and fused to a novel nucleic acid binding domain for improved isothermal amplification performance and increased reverse transcription activity. Bst 3.0 contains 5´→3´ DNA polymerase activity with either DNA or RNA templates and strong strand displacement activity but lacks 5´→3´ and 3´→5´ exonuclease activity. The polymerase has been tested to exhibit robust performance even in high concentrations of amplification inhibitors, and features significantly increased reverse transcriptase activity compared to wild type Bst DNA Polymerase [77]. Bst 2.0 DNA Polymerase contains 5´→3´ DNA polymerase activity and strong strand displacement activity but lacks 5´→3´ exonuclease activity. Bst 2.0 DNA Polymerase has been showed to display improved amplification speed, yield, salt tolerance and thermostability compared to wild-type Bst DNA Polymerase, Large Fragment [78] [79]. We tested Bst 3.0 in our reaction with blood plasma as sample matrix in which concentrations from 10^5 to 10^1 copies of HIV-1 was spiked.

We used WarmStart LAMP 2X Master Mix as a replacement to traditional Bst polymerase enzymes. The 2X master mix contains a blend of WarmStart Bst 2.0 DNA Polymerase and WarmStart RT enzyme in an optimized LAMP buffer solution containing dNTPs, MgSO4 [80]. The WarmStart master mix is also available in glycerol free form (GF), to accommodate lyophilization of reagents for incorporating in the device platform. The HIV-1 integrase RT-LAMP assay was tested for consistency under optimized condition and fresh reagents including GF-warm start master mix, dUTP, UDG and LAMP primers at 65^{o}C for 60 minutes.

3.3.3 HIV spiked in centrifuged plasma - in-tube amplification

Whole blood was diluted with a balanced salt solution; 1x Dulbecco's phosphate-buffered saline (DPBS) to obtain a final concentration of 5% and 10% plasma in reaction mixture. The diluted blood was centrifuged, and the resulting plasma supernatant was spiked with 4µL of HIV

template at final concentration of 2.5E5 vp/μL or 10^5 vp/rxn. 4 μL of DPBS was used as negative control to observe for non-specific amplification. The final volume in tubes was 25 μl - 17 μl master mix + 4 μl HIV spiked in sample matrix.

3.3.4 HIV spiked in plasma filtered through chip

Plasma was extracted by suspending DPBS (1x) diluted blood through a microfluidic chip. The push button in the microfluidic chip regulates the flow of blood extracting through the built-in filter in the chip, yielding plasma. HIV at $2.5x10^5$ vp/μL was spiked through 62.5% whole blood prior to filtration/extraction and isothermal assay performed to observe for amplification of controls. The final concentration of extracted plasma ~ 10% in 25 μL (4 μL of 62.5%). The assay was repeated my modifying assay conditions like 25% final concentration of plasma, whole blood diluted with 0.06x, 0.25x, 0.3x and 0.5x DPBS, whole blood diluted with water before filtration and using a 15 μL master mix volume and 10 μL template volume. The resulting LOD after blood separation and amplification with 0.06x DPBS was 10^5 vp/rxn, 0.3x at 25% plasma yielded no amplification, 0.5x at 25% plasma resulted in 10^4 vp/rxn. and 0.25x at 25% plasma dilution gave a slightly better recovery at 10^3 vp/rxn.

3.3.5 HIV spiked in lysed centrifuged whole blood - in-tube amplification

To minimize the sample preparation step for on-chip amplification in a point of care setting, we further explored lysing the whole blood with a suitable buffer cocktail prior to spiking with HIV. Protocol was adapted from a sensitivity detection study of Plasmodium Falciparum infection using RT-LAMP assay [81]. Blood cell lysis was achieved by mixing commercial patient blood samples (collected in K_3EDTA anticoagulant) with our in-house lysis buffer cocktail, containing 10 mM TRIS buffer (pH 7.4), 0.2% Bovine Serum Albumin (BSA), and 0.1% Triton-x-100. The mixture was centrifuged at 2000 x g for 10 minutes to separate the supernatant from the blood cell lysate. HIV template was serially diluted in the lysed blood from 10^5 vp/rxn through 10^1 vp/rxn. This was then spiked in the reaction followed by isothermal amplification and gel electrophoresis imaging.

Whole blood dilution with different ratios of lysis buffer

Whole blood was lysed with TBS cocktail at 1:2, 1:4, 1:6 and 1:8 ratio. The lysed blood was spiked with HIV template with the range of viral particle concentrations and streptavidin beads were added prior to isothermal amplification. Heating and amplification at 65°C for 60 minutes, produced nonspecific amplification of negative control (TBS cocktail in lysed blood) and amplification of all concentrations making the result inconclusive.

Comparison between HIV spiked in lysed blood and lysed centrifuged blood

To compare and determine a sample matrix for the LAMP assay, HIV template at different concentrations were spiked into different sample matrices. We tested plain lysis TB cocktail buffer (10 mM TRIS buffer, 0.2% BSA, 0.1% Triton X), whole blood lysed with the cocktail buffer, and supernatant obtained from centrifuging the lysed blood. HIV template was serially diluted with each of these matrices from 10^5 vp/rxn through 10^1 vp/rxn and spiked in the reaction mixture. To assess the sensitivity, we tried both 10% and 5% lysed blood concentrations and the assay was repeated thrice for consistency, and all were in-tube amplification spiked in plain lysis buffer, yielded a LOD of 10^3 vp/rxn at n=3 with no negative control amplification, LOD for HIV spiked in 10% lysed blood was 10^4 vp/rxn at n=3, with negative control amplifying once. LOD for HIV spiked in 5% lysed blood was inconclusive with a different LOD each time. HIV spiked in 5% lysed centrifuged blood was 10^3 vp/rxn twice and inconclusive the third time. The negative control amplification was due to prior hemolysis of blood when stored for a long period of time. Prior hemolysis of blood causes premature destruction of RBCs, and this could occur due to incorrect mixing and collection technique, improper storage and transportation conditions which results in a contamination in the solution. Since, we observed a lower LOD with 5% lysed centrifuged blood, we re-optimized the RT-LAMP assay to detect the HIV-1 integrase gene in 5% lysed centrifuged blood. The assay conditions were maintained at 65°C for 60 minutes and a comparison done by running the assay with and without adding streptavidin beads to the mixture. RT-LAMP assay with HIV spiked in 5% lysed centrifuged blood amplified with an LOD of 10^3 vp/rxn in tube. Due to COVID-19 pandemic, affecting material shipment, we could not gain access to blood collected in sodium citrate and therefore purchased blood collected in K_3EDTA (Tri-potassium Ethylenediaminetetraacetic acid).

3.3.6 HIV spiked in 5% lysed centrifuged blood with beads - in-tube amplification

We re-optimized the RT-LAMP assay to detect the HIV-1 integrase gene in 5% lysed centrifuged blood at 65°C for 60 minutes. Blood cell lysis was achieved by mixing commercial patient blood samples (collected in K_3EDTA anticoagulant) with our in-house lysis buffer cocktail, containing 10 mM Tris buffer (pH 7.4), 0.2% BSA, and 0.1% Triton-x-100. The mixture was then centrifuged at 2000 x g for 10 minutes to separate the supernatant from the blood cell lysate. HIV template was serially diluted in the supernatant of lysed centrifuged blood (5% final concentration) at concentrations 10^5 vp/rxn through 10^1 vp/rxn. 0.2mM $MgSO_4$ was added to the reaction mixture to compensate for the chelating effect of 0.2mM EDTA on Mg already present in the master mix. 400 nm streptavidin coated Dragon Green fluorescent particles were added to the reactions at a final concentration of prior to amplification. The final reaction volume of 25µl in tube contained – 17 µl master mix + 4µl (0.2mM $MgSO_4$) + 4µl template + 0.93µl (400 nm) streptavidin beads. LAMP amplicons were visualized using agarose gel electrophoresis and analyzed with smartphone-based PD-platform.

3.3.7 HIV spiked in 5% Lysed centrifuged blood with beads - on-chip amplification

The microfluidic chip comprises 3 main layers, a 1 mm thick microscope slide, 142 µm thick pressure sensitive adhesive (PSA), and a 50 µm thick cyclic olefin polymer (COP). A 15 µL microfluidic channel was patterned into the PSA layer and holes for the inlet, outlet, and extraction port cut into the COP layer using a laser cutter (VLS3.50, Universal Laser Systems Inc., Scottsdale, AZ, USA). A polydimethylsiloxane (PDMS) push button was used for fluid loading and extraction to drive the flow through the filter into the chip and extract the plasma. The push buttons were fabricated using Sylgard 184 (Dow Corning, Auburn, MI) mixed thoroughly in a standard 10:1 base: curing agent ratio that was degassed in a vacuum chamber for 10 to 15 minutes, poured over the push button master mold, before putting into an oven for 2 hours to bake at 55°C. The master mold consisted of an acrylic base with 1 mm thick acrylic cylinders applied with AR90880 PSA to secure and make 40 to 50µl push buttons. U-shaped chips - AR9880 (142 um thick) and AR92712 (50 um, stacked 3 times for 150 um) were used for the experiment. The final reaction volume and composition was same as in-tube amplification. A total of four chips with 2 NTC and 2 positive controls for each material type was tested. The chips were sealed with Bio-

Rad tape and heated ~65°C for 60 minutes and cooled for 10 minutes or more before imaging with PD platform. The solution from the chips were extracted using a pipette and visualized using agarose gel electrophoresis.

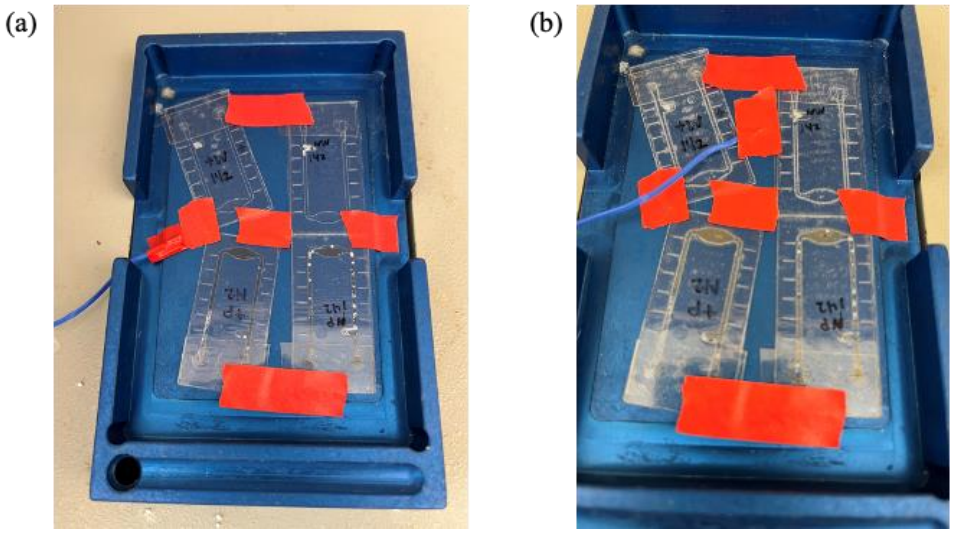

Figure 3.3- Chips placed on heat block at different time points. (a) t= 0 minutes on heat block, (b) t=60 minutes on heat block. Microchip fabrication and Image credits - Dr. Melinda Lake

3.3.8 Whole blood treatment for IgG and albumin removal

To observe for protein cloud formation, whole blood after lysis was pre-treated through an affinity column containing Albumin & IgG-Removal Resin. HIV particles were spiked in treated versus untreated 5% lysed blood. All reactions were prepared in tubes with same reaction and run time volume as above and loaded onto a thermally bonded COP chip for imaging under microscope setup.

3.3.9 HIV spiked in 5% Serum and 5% Plasma

We further investigated serum (Sigma Aldrich H3667) and plasma (extracted from blood samples with K_3EDTA anticoagulant through centrifugation) diluted in water (5% final concentration in reaction) to observe protein cloud formation.

3.4 Results and Discussion

3.4.1 Effect of re-designed *gag* and *int* primers in HIV amplification

The performance of the re-designed HIV-1 integrase gene primer set, and *gag* gene primer set was evaluated in a RT-LAMP reaction setup. The LOD with Gag primers and extracted plasma as sample matrix repeatedly was only 10^4 vp/rxn. Therefore, rest of the experiments were designed to detect the HIV-1 integrase gene.

3.4.2 Effect of different BST polymerases and enzymes in HIV amplification

While the BST3.0 was robust in the presence of plasma, we found that it presented false positive amplification in some of the negative controls. We tested the efficiency of Bst 2.0 polymerase in combination with Reverse Transcriptase (RTx) enzyme (New England Biolabs, Ipswich, MA). Upon testing the combination, Bst 2.0 polymerase did improve the non-specific amplification, but the enzyme was less robust to plasma. RT-LAMP assay using WarmStart RT-LAMP Master mix amplified 10^5 vp/reaction (25 µL reaction volume) in up to 10% plasma. We further incorporated dUTP and thermolabile Uracil DNA glycosylase (UDG) in the master mix to prevent carryover contamination. The assay provided a LOD of 10 vp/rxn and confirmed PD detection from plasma samples at in up to 10% plasma Figure 3.4. However, the LOD was not consistent upon further testing, but WarmStart RT-LAMP Master mix, UDG and dUTP were incorporated in reaction master mix.

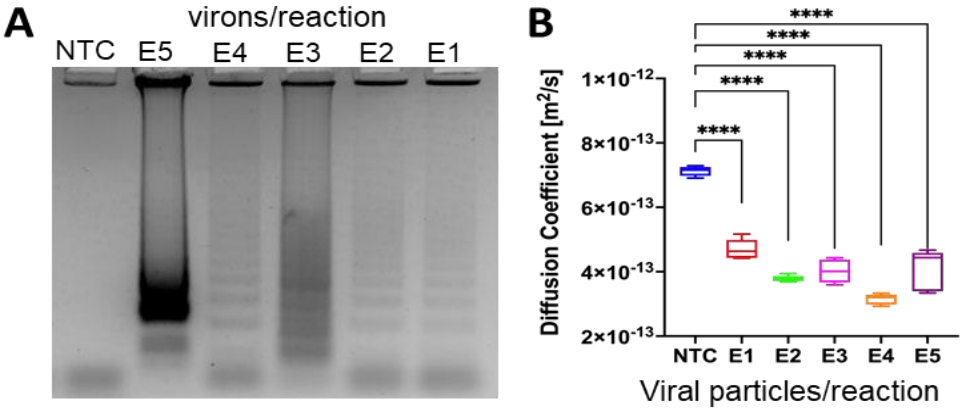

Figure 3.4. PD RT-LAMP in 10% plasma. LOD shown in (A) gel electrophoresis image and (B) PD results. The diffusion coefficient is significantly reduced in the HIV samples compared to the negative control (NTC) according to Dunnett's multiple comparison test (**** $p<0.0001$).

3.4.3 HIV spiked in centrifuged plasma - in-tube amplification

LAMP amplification and visualization through gel electrophoresis yielded no negative control amplification and a band for positive control at 10^5 vp/rxn. The limit of detection for the assay was 10^3 vp/rxn.

3.4.4 HIV spiked in plasma filtered through chip

The resulting LOD after blood separation and amplification with 0.06x DPBS was 10^5 vp/rxn, 0.3x at 25% plasma yielded no amplification, 0.5x at 25% plasma resulted in 10^4 vp/rxn. and 0.25x at 25% plasma dilution gave a slightly better recovery at 10^3 vp/rxn. Overall, it was observed that on increasing the template volume to 10 µL (25% plasma) provided a better LOD. Viscosity seemed to also play a role here, Lesser the viscosity, less was the bubble formation in chip, and it also seemed to improve sensitivity. Each of the above variations were tested in comparison with traditionally centrifuged plasma. However, the recovery of plasma through the chip was low compared to centrifugation process. Further to minimize same prep requirements under a point of care setting, we explored alternative options that allowed HIV amplification and reduced LOD.

3.4.5 HIV spiked in lysed centrifuged whole blood

As discussed above, we explored the idea of whole blood lysis with a suitable buffer cocktail prior to spiking with viral template to reduce steps in sample preparation. The whole blood with Sodium citrate as anticoagulant, was used for initial experiments. The blood was lysed with different ratios of TRIS buffer cocktail. Non-specific amplification of negative control (TBS cocktail in lysed blood) and amplification of all other positive concentrations were observed making the result inconclusive. The assay was further extended by performing a comparison between HIV spiked in lysed blood and lysed centrifuged blood to look for any artifact interference that might be leading to the inconclusive results. HIV-1 template spiked in plain TRIS buffer cocktail, yielded a LOD of 40 vp/µl at n=3 with no negative control amplification, indicating no inhibitors are present in the lysis buffer. LOD for HIV spiked in 10% lysed blood was 400vps/ µl at n=3, with negative control amplifying once. LOD for HIV spiked in 5% lysed blood was inconclusive with a different LOD at every repetition of experiment. HIV spiked in 5% lysed

centrifuged blood was 40 vps/µl twice and inconclusive the third time. The negative control amplification was due to prior hemolysis of blood when stored for a long period of time. Prior hemolysis of blood causes premature destruction of RBCs, and this could occur due to incorrect mixing and collection technique, improper storage and transportation conditions which results in a contamination in the solution. Since, we observed a lower LOD with 5% lysed centrifuged blood, we re-optimized the RT-LAMP assay to detect the HIV-1 integrase gene in 5% lysed centrifuged blood. The assay conditions were maintained at 65°C for 60 minutes and a comparison done by running the assay with and without adding streptavidin beads to the mixture. RT-LAMP assay with HIV spiked in 5% lysed centrifuged blood amplified with an LOD of 40 vp/µl in tube. Due to COVID-19 pandemic, affecting material shipment, we could not gain access to blood collected in sodium citrate and therefore purchased blood collected in K_3EDTA (Tri-potassium Ethylenediaminetetraacetic acid).

HIV spiked in 5% lysed centrifuged blood with beads - in-tube amplification

After re-optimizing the assay to detect HIV-1 integrase gene in 5% lysed centrifuged blood, we were able to bring down the LOD from 40 vp/µl to 25 vp/µl Figure 3.5. However, we could not get clear PD images for 25 vp/µl due to the protein clouds for the new LOD. Although, we demonstrated improved amplification via gel electrophoresis and a significant difference in the diffusion coefficients, we observed that the PD detection of amplicons was affected by blood protein coagulates forming clouds during the heating for the isothermal amplification. The protein clouds trap and hinder the motion of the detection particles (400 nm streptavidin particles) thereby, preventing accurate and consistent PD analysis Figure 3.6, C and D).

Troubleshooting protein cloud formation

The protein concentration in whole blood is about 60-80mg/ml. Out of this, 50–60% are albumins and 40% globulins, and 10-20% of these globulins are IgG [22]. To troubleshoot these reactions, we have evaluated whether the protein clouds form due to a) high total concentration of protein in the lysed blood being heated above the protein denaturing temperatures for 60 minutes, or b) a temperature-induced initiation of a clotting cascade. To test the total protein theory, we performed RT-LAMP in lysed blood pre-treated through an affinity column containing Albumin

& IgG-Removal Resin. HIV particles were spiked in treated versus untreated 5% lysed blood. All reactions were prepared in tubes and loaded onto a thermally bonded COP chip for imaging under microscope setup. Microscope setup was used for better resolution. No protein clouds were observed with treated blood; however, we observed particles settling at the bottom of the chip (Figure 3. 4 E and F) during the reaction which would prohibit real-time diffusivity quantification. We further tested using a commercially obtained RBC lysis buffer [83] and an in-house ammonium chloride lysis buffer [84] as alternative options of efficient whole blood lysis. However, even they seemed to not improve the cloud formation.

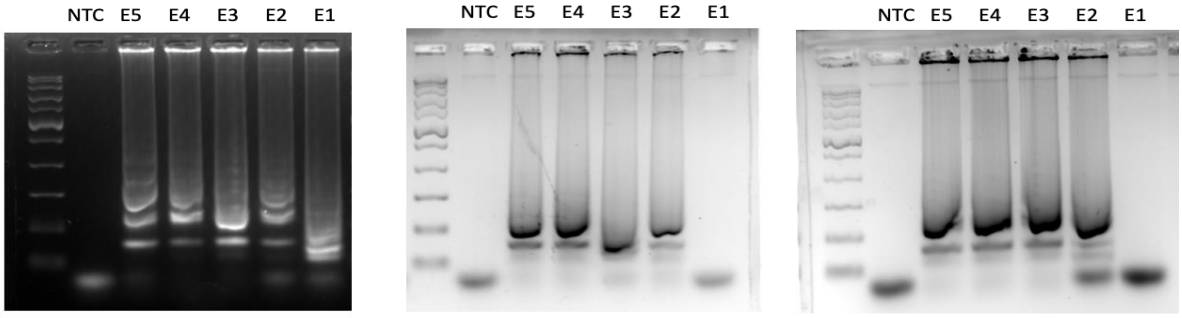

Figure 3.5. RT-LAMP in 5% lysed centrifuged blood demonstrates amplification of as little as 25 viral copies/µl in gel electrophoresis at n= 3.

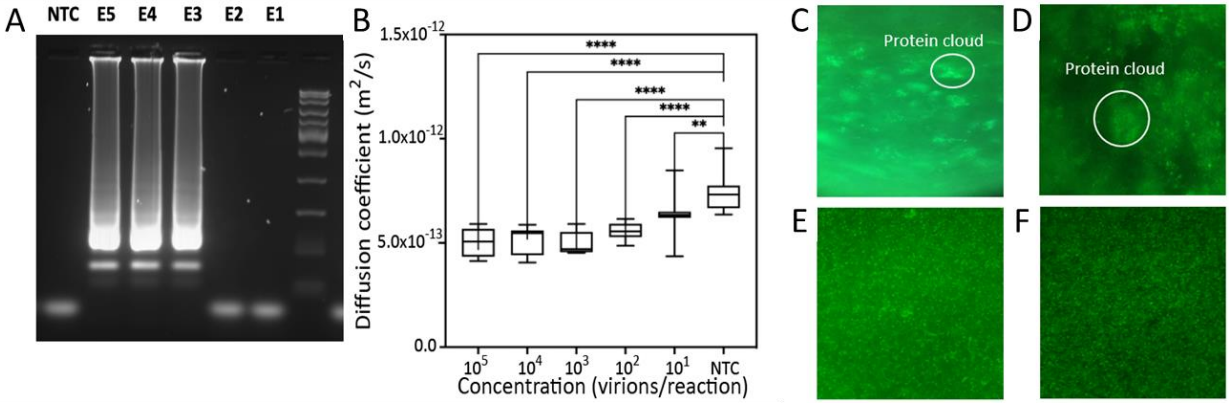

Figure 3.6. RT-LAMP in 5% lysed centrifuged blood demonstrates amplification of as little as 40 viral copies/µl in gel electrophoresis (A) and PD (B). The diffusion coefficient is reduced in the HIV samples compared to the negative control (NTC) according to Dunnett's multiple comparison test (**** $p<0.0001$, ** $p<0.01$). (C-F) Comparative results displaying protein cloud and steps to remove the protein cloud in 5% lysed blood. Images of particles in the middle of the imaging chambers without igg/Albumin removal in (C) NTC and (D) 105 virons/µl. Images from the bottom of the chamber with igg/Albumin removal in (E) NTC and (F) 10^5vp/rxn.

3.4.6 HIV spiked in 5% Serum and 5% Plasma

The results were promising with no sedimentation of particles, and no clouds observed with both Serum and Plasma under PD imaging which is promising, and diffusion coefficient values also showed statistical significance between NTC and E5. Unfortunately, the LOD was 4000vp/µl, which is very high Figure 3.7. At present, both plasma and serum appear to be appropriate sample matrix, however, the LOD in plasma and serum was not sufficient and requires further optimization and both sample matrices require longer separation from whole blood.

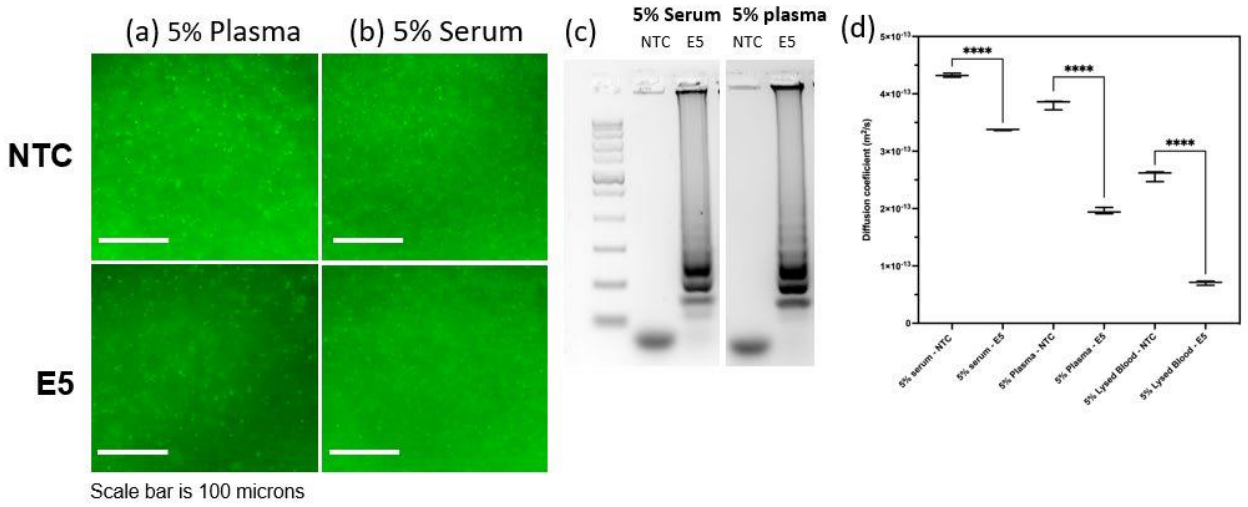

Figure 3.7. Serum (5%), plasma (5%), and lysed blood (5%) amplification results. Smartphone images of (a) beads in serum samples in NTC and 105 virions/reaction, (b) in plasma samples in NTC and 105 virions/reaction, and (c) in lysed blood samples NTC and 105 virions/reaction. (c) Gel electrophoresis results. (d) Diffusion coefficient values for NTC and 105 virions/reaction samples for HIV spiked in serum, plasma, and lysed blood, respectively.

3.5 Conclusion and future directions

The RT-LAMP assay parameters have been optimized to yield a LOD of 25 vp/µl from whole blood in tube. However, this assay has not been successful when imaged under the PD platform due to the formation of protein clouds and sedimentation of particles. The clouds and streptavidin beads settling down at the bottom of the chip impair the particle movement and the diffusion coefficient values generated are therefore, inconsistent, and inconclusive for positive results. Potential alternative solutions are working on HIV enrichment techniques using filtering paper to achieve an improved LOD.

4. CONCLUSION AND FUTURE DIRECTIONS

In chapter 2, we have successfully compared the binding kinetics of p24 Ab to p24 Ag and quantified this binding via Bio-Layer Interferometry measurements. We have tested the binding affinity of 8 different mouse monoclonal antibodies to p24 Ag, both individually and in a tandem format (pair of Ab and Ag). The study has provided us with antibodies that are able to rapidly bind to its target p24 Ag, and pair of antibodies with dual recognition. Dual recognition will allow detection of multiple epitopes on the site of target antigen. This is essential for when detection by single epitope binding fails. Additionally, when dual recognition incorporated in immuno-assay formats will also reduce the number of false positives. Going forward this work will be continued using the choice of Antibody pair to design and optimize the ai-LAMP assay design. Currently, the binding data from all antibodies is being used to perform a dot-blot for additional antibody screening, to make a lateral flow assay test for early HIV detection using HRP signal enhancement.

In chapter 3, we have successfully validated the working primer design for target region specificity, optimized limit of detection in whole blood, and optimized reaction mixture composition. We now have a HIV-PD-RT-LAMP assay functional at 5% lysed blood to detcet integrase gene down to 100 vp/rxn (25 vp/µl) without any nonspecific amplification. The assay has been validated using gel electrophoresis for consistency. There are several ways to move forward with aim 2. As, plasma and serum proved to be appropriate sample matrices for no cloud formation, we could work on additional sample processing requirements for both. Sample processing here would be figuring out ways to reduce separation time from whole blood to be compatible with point of use requirements. An alternative way to refine the the process of HIV detection is use extraction paper-based enrichment techniques for usability in a point of care setting. Paper based diagnostics is easy to use and interpret, cost-effective and scalable. Here, enrichment strategy is using filter paper to capture the HIV RNA released into the sample after cell lysis. Since nucleic acids bind to cellulose fibers so both human DNA and viral RNA will bind to the paper membrane, and we can then process bound paper for selective detection of RNA.

APPENDIX A. SUPPPLEMENT TO CHAPTER 2

Protocol A.1 - Steps for Ligand-Analyte Binding on Octet 384

i. Pre-hydrated 16 different HIS1K biosensors in the rack with a 96-well black plate containing 200 µL/well 1X KB, for at least 10 min at 30°C.

ii. Diluted HIV P24 Ag in 1X KB to a final volume of 200 µL/well at a concentration of 10 µg/ml.

iii. Control wells (a 0nM Ab well and 20nM Ab with 0 µg/ml antigen) filled with 200 µL of 1X KB and the baseline columns were suspended with the same volume of 1X KB to account for nonspecific binding of Ab to the biosensor.

iv. Titrated Abs with 1X KB (200 µL for each concentration) in three-fold serial dilutions - 20nM, 6.7nM, 2.2nM, 0.73nM, 0.25nM, 0.1nM.

v. The assay steps listed below were followed throughout for all ligand-analyte combinations

- Baseline: 120 s
- Loading: 160 s
- Wash: 120
- Baseline: 120 s
- Association: 300 s
- Dissociation: 600 s

vi. Captured p24 using HIS1K biosensors, followed by a brief wash and baseline stabilization in 1X KB.

vii. Submerged the p24 Ag-captured biosensors in different concentrations of Abs for 5 mins followed by 10 mins of dissociation time in 1X KB.

viii. 8-channel detection mode was used to collect the binding sensorgram and fresh HIS1K biosensors, ligands, and analyte was used without any regeneration.

ix. Data processed and analyzed.

Protocol A.2 - Steps for Ligand-Analyte Binding on Octet 384

i. 8 different HIS1K biosensors were pre-hydrated in the biosensor rack with a 96-well black plate containing 200 µL/well 1X KB, for at least 10 min at 30°C.

ii. The assay parameters, dilution volume, and concentrations remain the same for Ag.

iii. We tested binding interaction between mAB247P (Ab1) and 4 other Abs as Ab2 (mAB246P, MAB248P, mAB249P, and J317). Based on the previous analyte binding study, a concentration that yielded a strong KD value along with stable on and off rates is ideal to use for both Abs in this study. Based on that, we chose to run both Abs at a 6.7nM concentration and each Ab was titrated with 1X KB (200 µL for each well)

iv. In the presence of second Ab (Ab2), we introduce a second wash and baseline step after the dissociation of Ab2, to allow the binding of Ab2 with minimum baseline drift and specificity. The step times are listed below in respective order -

- Baseline: 120 s
- Loading: 160 s
- Wash: 120
- Baseline: 120 s
- Association: 300 s
- Dissociation: 600 s
- Wash: 120
- Baseline: 120 s
- Association: 300 s
- Dissociation: 600 s

v. To account for background drift and binding accuracy, Ag-loaded biosensors are dipped into control wells with either media or buffer instead of Ab1, and then into all competing antibodies (Ab2). This helps to determine the extent of each Ab2 binding to the antigen in the absence of Ab1.

vi. After an initial baseline step, the binding kinetics study proceeded by first capturing p24 Ag using HIS1K biosensors followed by a brief wash and baseline stabilization in 1X KB. The p24 Ag-captured biosensors were then submerged in wells containing 6.7nM of Ab1 for 5 mins followed by 10 mins of dissociation time in 1X KB. Once Ab1 reaches

saturation, the second wash and baseline steps were performed, and the second association and dissociation were run with four different Ab2s.

vii. The binding sensorgram was collected using the high sensitivity 8-channel detection mode on the Octet RED384 biosensor. Fresh HIS1K biosensors, ligands, and analytes were used without any regeneration.

viii. Data processed and analyzed.

Table A.1 *KD* values for different concentrations of mAB246P, mAB247P, mAB248P, mAB249P

mAB248P

	Sensor Type	Loading Sample ID	Sample ID	Conc. (nM)	KD (M)	kon(1/Ms)	kdis(1/s)	Full R^2
1	HIS1K (Anti-Pen	HIV1-HXB2-P24	mAB248P	20	<1.0E-12	2.35E+05	<1.0E-07	0.9953
2	HIS1K (Anti-Pen	HIV1-HXB2-P24	mAB248P	6.7	<1.0E-12	3.15E+05	<1.0E-07	0.9923
3	HIS1K (Anti-Pen	HIV1-HXB2-P24	mAB248P	2.2	1.36E-10	6.27E+05	8.51E-05	0.9949
4	HIS1K (Anti-Pen	HIV1-HXB2-P24	mAB248P	0.74	1.99E-09	1.17E+05	2.31E-04	0.9359
5	HIS1K (Anti-Pen	HIV1-HXB2-P24	mAB248P	0.247	<1.0E-12	2.52E+06	<1.0E-07	0.5774
6	HIS1K (Anti-Pen	HIV1-HXB2-P24	mAB248P	0.1	<1.0E-12	7.03E+06	<1.0E-07	0.5434
7	HIS1K (Anti-Pen	HIV1-HXB2-P24	mAB248P	20	<1.0E-12	2.35E+05	<1.0E-07	0.9953
8	HIS1K (Anti-Pen	HIV1-HXB2-P24	mAB248P	6.7	<1.0E-12	3.15E+05	<1.0E-07	0.9923
9	HIS1K (Anti-Pen	HIV1-HXB2-P24	mAB248P	2.2	1.36E-10	6.27E+05	8.51E-05	0.9949
10	HIS1K (Anti-Pen	HIV1-HXB2-P24	mAB248P	0.74	1.99E-09	1.17E+05	2.31E-04	0.9359
11	HIS1K (Anti-Pen	HIV1-HXB2-P24	mAB248P	0.247	<1.0E-12	2.52E+06	<1.0E-07	0.5774
12	HIS1K (Anti-Pen	HIV1-HXB2-P24	mAB248P	0.1	<1.0E-12	7.03E+06	<1.0E-07	0.5434

mAB246P

	Sensor Type	Loading Sample ID	Sample ID	Conc. (nM)	KD (M)	kon(1/Ms)	kdis(1/s)	Full R^2
1	HIS1K (Anti-Pen	HIV1-HXB2-P24	mAB246P	20	<1.0E-12	2.65E+05	<1.0E-07	0.9909
2	HIS1K (Anti-Pen	HIV1-HXB2-P24	mAB246P	6.67	<1.0E-12	4.97E+05	<1.0E-07	0.985
3	HIS1K (Anti-Pen	HIV1-HXB2-P24	mAB246P	2.2	5.28E-12	1.75E+06	9.21E-06	0.9896
4	HIS1K (Anti-Pen	HIV1-HXB2-P24	mAB246P	0.74	<1.0E-12	4.94E+06	<1.0E-07	0.9843
5	HIS1K (Anti-Pen	HIV1-HXB2-P24	mAB246P	0.247	3.49E-11	5.19E+07	1.81E-03	0.6597
6	HIS1K (Anti-Pen	HIV1-HXB2-P24	mAB246P	0.1	8.47E-12	8.75E+07	7.41E-04	0.7239
7	HIS1K (Anti-Pen	HIV1-HXB2-P24	mAB246P	20	<1.0E-12	2.65E+05	<1.0E-07	0.9909
8	HIS1K (Anti-Pen	HIV1-HXB2-P24	mAB246P	6.67	<1.0E-12	4.97E+05	<1.0E-07	0.985
9	HIS1K (Anti-Pen	HIV1-HXB2-P24	mAB246P	2.2	5.28E-12	1.75E+06	9.21E-06	0.9896
10	HIS1K (Anti-Pen	HIV1-HXB2-P24	mAB246P	0.74	<1.0E-12	4.94E+06	<1.0E-07	0.9843
11	HIS1K (Anti-Pen	HIV1-HXB2-P24	mAB246P	0.247	3.49E-11	5.19E+07	1.81E-03	0.6597
12	HIS1K (Anti-Pen	HIV1-HXB2-P24	mAB246P	0.1	8.47E-12	8.75E+07	7.41E-04	0.7239

mAB247P

	Sensor Type	Loading Sample	Sample ID	Conc. (nM)	KD (M)	kon(1/Ms)	kdis(1/s)	Full R^2
1	HIS1K (Anti-Pen	HIV1-HXB2-P24	mAB-247P	20	<1.0E-12	4.27E+05	<1.0E-07	0.9985
2	HIS1K (Anti-Pen	HIV1-HXB2-P24	mAB-247P	6.67	<1.0E-12	5.16E+05	<1.0E-07	0.9919
3	HIS1K (Anti-Pen	HIV1-HXB2-P24	mAB-247P	2.2	<1.0E-12	8.11E+05	<1.0E-07	0.9924
4	HIS1K (Anti-Pen	HIV1-HXB2-P24	mAB-247P	0.73	3.53E-11	1.25E+06	4.41E-05	0.9974
5	HIS1K (Anti-Pen	HIV1-HXB2-P24	mAB-247P	0.25	9.50E-11	8.28E+06	7.87E-04	0.9769
6	HIS1K (Anti-Pen	HIV1-HXB2-P24	mAB-247P	0.1	2.30E-10	8.78E+05	2.02E-04	0.8956
7	HIS1K (Anti-Pen	HIV1-HXB2-P24	mAB-247P	20	<1.0E-12	4.27E+05	<1.0E-07	0.9985
8	HIS1K (Anti-Pen	HIV1-HXB2-P24	mAB-247P	6.67	<1.0E-12	5.16E+05	<1.0E-07	0.9919
9	HIS1K (Anti-Pen	HIV1-HXB2-P24	mAB-247P	2.2	<1.0E-12	8.11E+05	<1.0E-07	0.9924
10	HIS1K (Anti-Pen	HIV1-HXB2-P24	mAB-247P	0.73	3.53E-11	1.25E+06	4.41E-05	0.9974
11	HIS1K (Anti-Pen	HIV1-HXB2-P24	mAB-247P	0.25	9.50E-11	8.28E+06	7.87E-04	0.9769
12	HIS1K (Anti-Pen	HIV1-HXB2-P24	mAB-247P	0.1	2.30E-10	8.78E+05	2.02E-04	0.8956

mAB249P

1	Sensor Type	Loading Sample ID	Sample ID	Conc. (nM)	KD (M)	kon(1/Ms)	kdis(1/s)	Full R^2
2	HIS1K (Anti-Penta	HIV1-HXB2-P24	mAB249P	20	<1.0E-12	1.78E+05	<1.0E-07	0.9878
3	HIS1K (Anti-Penta	HIV1-HXB2-P24	mAB249P	6.67	<1.0E-12	3.55E+05	<1.0E-07	0.9526
4	HIS1K (Anti-Penta	HIV1-HXB2-P24	mAB249P	2.2	<1.0E-12	1.73E+06	<1.0E-07	0.8511
5	HIS1K (Anti-Penta	HIV1-HXB2-P24	mAB249P	0.6667	<1.0E-12	4.08E+06	<1.0E-07	0.605
6	HIS1K (Anti-Penta	HIV1-HXB2-P24	mAB249P	0.2467	<1.0E-12	9.20E+06	<1.0E-07	0.4263
7	HIS1K (Anti-Penta	HIV1-HXB2-P24	mAB249P	0.1	<1.0E-12	1.00E+08	<1.0E-07	0
8	HIS1K (Anti-Penta	HIV1-HXB2-P24	mAB249P	20	<1.0E-12	1.78E+05	<1.0E-07	0.9878
9	HIS1K (Anti-Penta	HIV1-HXB2-P24	mAB249P	6.67	<1.0E-12	3.55E+05	<1.0E-07	0.9526
10	HIS1K (Anti-Penta	HIV1-HXB2-P24	mAB249P	2.2	<1.0E-12	1.73E+06	<1.0E-07	0.8511
11	HIS1K (Anti-Penta	HIV1-HXB2-P24	mAB249P	0.6667	<1.0E-12	4.08E+06	<1.0E-07	0.605
12	HIS1K (Anti-Penta	HIV1-HXB2-P24	mAB249P	0.2467	<1.0E-12	9.20E+06	<1.0E-07	0.4263
13	HIS1K (Anti-Penta	HIV1-HXB2-P24	mAB249P	0.1	<1.0E-12	1.00E+08	<1.0E-07	0

Table A.2 KD values for different concentrations of ECB - J317, FITZ-10-1525, FITZ-10-2842,FITZ-10-2843

ECB-J317

	Sensor Type	Loading Sample ID	Sample ID	KD (M)	Conc. (nM)	kon(1/Ms)	kdis(1/s)	Full R^2
1	HIS1K (Anti-Penta	HIV1-HXB2-P24	EABJ317	<1.0E-12	20	4.80E+05	<1.0E-07	0.9953
2	HIS1K (Anti-Penta	HIV1-HXB2-P24	EABJ317	<1.0E-12	6.67	5.74E+05	<1.0E-07	0.995
3	HIS1K (Anti-Penta	HIV1-HXB2-P24	EABJ317	<1.0E-12	2.2	1.23E+06	<1.0E-07	0.9786
4	HIS1K (Anti-Penta	HIV1-HXB2-P24	EABJ317	<1.0E-12	0.74	2.37E+06	<1.0E-07	0.9602
5	HIS1K (Anti-Penta	HIV1-HXB2-P24	EABJ317	1.42E-11	0.2467	2.92E+07	4.14E-04	0.6227
6	HIS1K (Anti-Penta	HIV1-HXB2-P24	EABJ317	6.06E-11	0.1	1.75E+07	1.06E-03	0.9367
7	HIS1K (Anti-Penta	HIV1-HXB2-P24	EABJ317	<1.0E-12	20	4.80E+05	<1.0E-07	0.9953
8	HIS1K (Anti-Penta	HIV1-HXB2-P24	EABJ317	<1.0E-12	6.67	5.74E+05	<1.0E-07	0.995
9	HIS1K (Anti-Penta	HIV1-HXB2-P24	EABJ317	<1.0E-12	2.2	1.23E+06	<1.0E-07	0.9786
10	HIS1K (Anti-Penta	HIV1-HXB2-P24	EABJ317	<1.0E-12	0.74	2.37E+06	<1.0E-07	0.9602
11	HIS1K (Anti-Penta	HIV1-HXB2-P24	EABJ317	1.42E-11	0.2467	2.92E+07	4.14E-04	0.6227
12	HIS1K (Anti-Penta	HIV1-HXB2-P24	EABJ317	6.06E-11	0.1	1.75E+07	1.06E-03	0.9367

FITZ-10-1525

	Sensor Type	Loading Sample ID	Sample ID	Conc. (nM)	KD (M)	kon(1/Ms)	kdis(1/s)	Full R^2
1	HIS1K (Anti-Penta	HIV1-HXB2-P24	FITZ-10-2842	20	1.40E-12	5.02E+05	7.00E-07	0.9989
2	HIS1K (Anti-Penta	HIV1-HXB2-P24	FITZ-10-2842	6.67	<1.0E-12	5.42E+05	<1.0E-07	0.9954
3	HIS1K (Anti-Penta	HIV1-HXB2-P24	FITZ-10-2842	2.2	<1.0E-12	5.64E+05	<1.0E-07	0.9917
4	HIS1K (Anti-Penta	HIV1-HXB2-P24	FITZ-10-2842	0.6667	<1.0E-12	1.67E+06	<1.0E-07	0.9612
5	HIS1K (Anti-Penta	HIV1-HXB2-P24	FITZ-10-2842	0.2467	2.58E-11	7.86E+06	2.03E-04	0.785
6	HIS1K (Anti-Penta	HIV1-HXB2-P24	FITZ-10-2842	0.1	<1.0E-12	2.41E+07	<1.0E-07	0.4804
7	HIS1K (Anti-Penta	HIV1-HXB2-P24	FITZ-10-2842	20	1.40E-12	5.02E+05	7.00E-07	0.9989
8	HIS1K (Anti-Penta	HIV1-HXB2-P24	FITZ-10-2842	6.67	<1.0E-12	5.42E+05	<1.0E-07	0.9954
9	HIS1K (Anti-Penta	HIV1-HXB2-P24	FITZ-10-2842	2.2	<1.0E-12	5.64E+05	<1.0E-07	0.9917
10	HIS1K (Anti-Penta	HIV1-HXB2-P24	FITZ-10-2842	0.6667	<1.0E-12	1.67E+06	<1.0E-07	0.9612
11	HIS1K (Anti-Penta	HIV1-HXB2-P24	FITZ-10-2842	0.2467	2.58E-11	7.86E+06	2.03E-04	0.785
12	HIS1K (Anti-Penta	HIV1-HXB2-P24	FITZ-10-2842	0.1	<1.0E-12	2.41E+07	<1.0E-07	0.4804

FITZ-10-2842

	Sensor Type	Loading Sample ID	Sample ID	Conc. (nM)	KD (M)	kon(1/Ms)	kdis(1/s)	Full R^2
1	HIS1K (Anti-Penta	HIV1-HXB2-P24	FITZ-10-1525	20	<1.0E-12	4.53E+05	<1.0E-07	0.9932
3	HIS1K (Anti-Penta	HIV1-HXB2-P24	FITZ-10-1525	6.67	<1.0E-12	5.41E+05	<1.0E-07	0.9916
4	HIS1K (Anti-Penta	HIV1-HXB2-P24	FITZ-10-1525	2.2	<1.0E-12	5.59E+05	<1.0E-07	0.9815
5	HIS1K (Anti-Penta	HIV1-HXB2-P24	FITZ-10-1525	0.74	<1.0E-12	1.29E+06	<1.0E-07	0.9078
6	HIS1K (Anti-Penta	HIV1-HXB2-P24	FITZ-10-1525	0.2467	<1.0E-12	9.29E+06	<1.0E-07	0.539
7	HIS1K (Anti-Penta	HIV1-HXB2-P24	FITZ-10-1525	0.1	<1.0E-12	1.00E+08	<1.0E-07	0
8	HIS1K (Anti-Penta	HIV1-HXB2-P24	FITZ-10-1525	20	<1.0E-12	4.53E+05	<1.0E-07	0.9932
9	HIS1K (Anti-Penta	HIV1-HXB2-P24	FITZ-10-1525	6.67	<1.0E-12	5.41E+05	<1.0E-07	0.9916
10	HIS1K (Anti-Penta	HIV1-HXB2-P24	FITZ-10-1525	2.2	<1.0E-12	5.59E+05	<1.0E-07	0.9815
11	HIS1K (Anti-Penta	HIV1-HXB2-P24	FITZ-10-1525	0.74	<1.0E-12	1.29E+06	<1.0E-07	0.9078
12	HIS1K (Anti-Penta	HIV1-HXB2-P24	FITZ-10-1525	0.2467	<1.0E-12	9.29E+06	<1.0E-07	0.539
13	HIS1K (Anti-Penta	HIV1-HXB2-P24	FITZ-10-1525	0.1	<1.0E-12	1.00E+08	<1.0E-07	0

FITZ-10-2843

	Sensor Type	Loading Sample ID	Sample ID	Conc. (nM)	KD (M)	kon(1/Ms)	kdis(1/s)	Full R^2
1	HIS1K (Anti-Pent	HIV1-HXB2-P24	FITZ-10-2843	20	<1.0E-12	6.05E+05	<1.0E-07	0.991
2	HIS1K (Anti-Pent	HIV1-HXB2-P24	FITZ-10-2843	6.67	<1.0E-12	5.26E+05	<1.0E-07	0.9918
3	HIS1K (Anti-Pent	HIV1-HXB2-P24	FITZ-10-2843	2.2	<1.0E-12	1.05E+06	<1.0E-07	0.9496
4	HIS1K (Anti-Pent	HIV1-HXB2-P24	FITZ-10-2843	0.6667	<1.0E-12	1.90E+06	<1.0E-07	0.8484
5	HIS1K (Anti-Pent	HIV1-HXB2-P24	FITZ-10-2843	0.2467	<1.0E-12	9.20E+06	<1.0E-07	0.7121
6	HIS1K (Anti-Pent	HIV1-HXB2-P24	FITZ-10-2843	0.1	<1.0E-12	1.00E+08	<1.0E-07	0
7	HIS1K (Anti-Pent	HIV1-HXB2-P24	FITZ-10-2843	20	<1.0E-12	6.05E+05	<1.0E-07	0.991
8	HIS1K (Anti-Pent	HIV1-HXB2-P24	FITZ-10-2843	6.67	<1.0E-12	5.26E+05	<1.0E-07	0.9918
9	HIS1K (Anti-Pent	HIV1-HXB2-P24	FITZ-10-2843	2.2	<1.0E-12	1.05E+06	<1.0E-07	0.9496
10	HIS1K (Anti-Pent	HIV1-HXB2-P24	FITZ-10-2843	0.6667	<1.0E-12	1.90E+06	<1.0E-07	0.8484
11	HIS1K (Anti-Pent	HIV1-HXB2-P24	FITZ-10-2843	0.2467	<1.0E-12	9.20E+06	<1.0E-07	0.7121
12	HIS1K (Anti-Pent	HIV1-HXB2-P24	FITZ-10-2843	0.1	<1.0E-12	1.00E+08	<1.0E-07	0

APPENDIX B. SUPPLEMENT TO CHAPTER 3

Table B.1 HIV-1 LAMP primers

Primers targeting Gag gene of HIV-1

Primer	Sequence (5' – 3')
F3	TCAGCATTATCAGAAGGAGC
B3	AGTTCCTGCTATGTCACTTC
BIP	GGTCTCTTTTAACATTTGCATGGCTTTTTTTAAACACCATGCTAAACACA
FIP	ATGAGGAAGCTGCAGAATGGGTTTTCCCTTGGTTCTCTCATCTG
LB	TGCTTGATGTCCCCCCAC
LF	AGTGCATGCAGGGCCTATTG
LF-S9	/5BiosG/iSp9/TGCTTGATGTCCCCCCAC
LF-Biotin	/5BioTinTEG/TGCTTGATGTCCCCCCAC

Table B.2 HIV-1 LAMP primers

Primers targeting Integrase gene of HIV-1

Primer	Sequence (5' – 3')
F3	GGTAAGAGATCAGGCTGAACATC
B3	TTTGCTGGTCCTTTCCAAAG
FIP	CCC CAA TCC CCC CTT TAA GAC AGC AGT ACA AAT GGC AG
BIP	AGT GCA GGG GAA AGA ATA GTA GAC CTG CTG TCC CTG TAA TAA ACC C
LF	GCAACAGACATACAAACTAAAG
LB	TTAAAATTGTGGATGAAT
LF-Biotin	/5Biosg/TTAAAATTGTGGATGAAT

Table B.3 Optimized RT-LAMP master mix for HIV-1

Reagent	Final concentration
dUTP (100 mM)	700 µM
UDG	1X
F3 primer (100 µM)	0.2 µM
B3 primer (100 µM)	0.2 µM
FIP primer (100 µM)	1.6 µM
BIP primer (100 µM)	1.6 µM
LF primer (100 µM)	0.4 µM
LB primer (100 µM)	0.4 µM
WarmStart HIV-RT-LAMP 2X Master Mix	1x

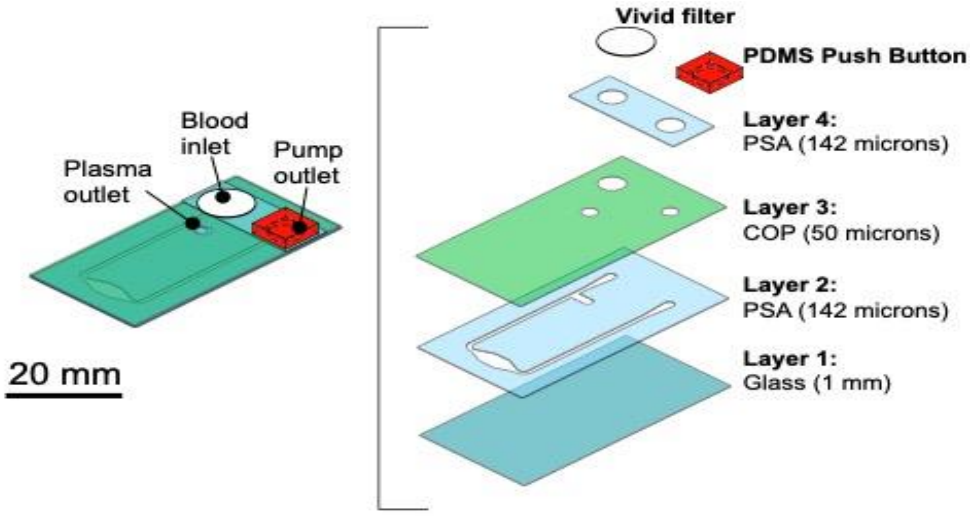

Figure B.1 Single Microchip chamber
Credits - Dr. Melinda Lake, Linnes lab

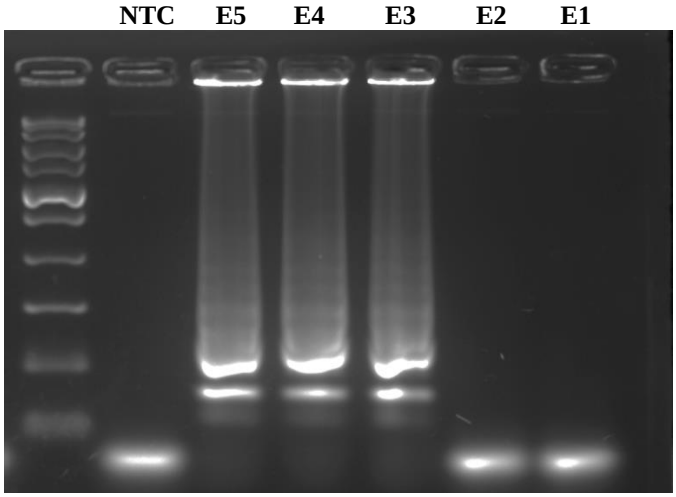

Figure B.2 Gel electrophoresis results showing removal of Eva Green and ROX dye does not alter the LOD

REFERENCES

[1] “hiv and aids - basic facts.” Https://www.unaids.org/en/frequently-asked-questions-about-hiv-and-aids (accessed nov. 12, 2022).

[2] g. A. C. B. (arbeitskreis blut) and s. ‘assessment of p. T. By blood’, “human immunodeficiency virus (hiv),” tmh, vol. 43, no. 3, pp. 203–222, 2016, doi: 10.1159/000445852.

[3] y. Van heuvel, s. Schatz, j. F. Rosengarten, and j. Stitz, “infectious rna: human immunodeficiency virus (hiv) biology, therapeutic intervention, and the quest for a vaccine,” toxins, vol. 14, no. 2, art. No. 2, feb. 2022, doi: 10.3390/toxins14020138.

[4] “cd4 t lymphocyte | nih.” Https://clinicalinfo.hiv.gov/en/glossary/cd4-t-lymphocyte (accessed nov. 01, 2022).

[5] “the hiv life cycle | nih.” Https://hivinfo.nih.gov/understanding-hiv/fact-sheets/hiv-life-cycle (accessed nov. 01, 2022).

[6] “hiv.” Https://www.who.int/news-room/fact-sheets/detail/hiv-aids (accessed nov. 01, 2022).

[7] “symptoms of hiv,” hiv.gov. Https://www.hiv.gov/hiv-basics/overview/about-hiv-and-aids/symptoms-of-hiv (accessed nov. 01, 2022).

[8] “the stages of hiv infection | nih.” Https://hivinfo.nih.gov/understanding-hiv/fact-sheets/stages-hiv-infection (accessed sep. 26, 2022).

[9] “centralized vs. Decentralized testing models and the importance of both for covid-19 testing,” diagnostics. Https://diagnostics.roche.com/us/en/article-listing/centralized-vs-decentralized-testing-models-and-the-importance-o.html (accessed nov. 01, 2022).

[10] “detection of acute hiv infection | the journal of infectious diseases | oxford academic.” Https://academic.oup.com/jid/article/202/supplement_2/s270/852813 (accessed nov. 01, 2022).

[11] “point-of-care testing (poct),” point-of-care testing (poct). Https://ncpa.org/point-care-testing-poct (accessed nov. 03, 2022).

[12] h.-d. Park, “current status of clinical application of point-of-care testing,” archives of pathology & laboratory medicine, vol. 145, no. 2, pp. 168–175, oct. 2020, doi: 10.5858/arpa.2020-0112-ra.

[13] "global point of care diagnostics market forecast to reach $43.5 billion by 2026 - researchandmarkets.com," dec. 29, 2021. Https://www.businesswire.com/news/home/20211229005194/en/global-point-of-care-diagnostics-market-forecast-to-reach-43.5-billion-by-2026---researchandmarkets.com (accessed nov. 03, 2022).

[14] a. Bernabé-ortiz et al., "diagnostics and monitoring tools for noncommunicable diseases: a missing component in the global response," globalization and health, vol. 17, no. 1, p. 26, mar. 2021, doi: 10.1186/s12992-021-00676-6.

[15] a. St john and c. P. Price, "existing and emerging technologies for point-of-care testing," clin biochem rev, vol. 35, no. 3, pp. 155–167, aug. 2014.

[16] m. K. Haleyur giri setty and i. K. Hewlett, "point of care technologies for hiv," aids research and treatment, vol. 2014, p. E497046, jan. 2014, doi: 10.1155/2014/497046.

[17] a. F. A. Meyers et al., "quality assurance for hiv point-of-care testing and treatment monitoring assays," afr j lab med, vol. 5, no. 2, p. 557, oct. 2016, doi: 10.4102/ajlm.v5i2.557.

[18] s. Sachdeva, r. W. Davis, and a. K. Saha, "microfluidic point-of-care testing: commercial landscape and future directions," frontiers in bioengineering and biotechnology, vol. 8, 2021, accessed: nov. 03, 2022. [online]. Available: https://www.frontiersin.org/articles/10.3389/fbioe.2020.602659

[19] v. Naresh and n. Lee, "a review on biosensors and recent development of nanostructured materials-enabled biosensors," sensors, vol. 21, no. 4, art. No. 4, jan. 2021, doi: 10.3390/s21041109.

[20] f. Guan et al., "preparation of hydrophobic transparent paper via using polydimethylsiloxane as transparent agent," journal of bioresources and bioproducts, vol. 5, no. 1, pp. 37–43, feb. 2020, doi: 10.1016/j.jobab.2020.03.004.

[21] y. Xie, l. Dai, and y. Yang, "microfluidic technology and its application in the point-of-care testing field," biosens bioelectron x, vol. 10, p. 100109, may 2022, doi: 10.1016/j.biosx.2022.100109.

[22] s. Das, d. R. Shibib, and m. O. Vernon, "the new frontier of diagnostics: molecular assays and their role in infection prevention and control," am j infect control, vol. 45, no. 2, pp. 158–169, feb. 2017, doi: 10.1016/j.ajic.2016.08.005.

[23] k. Mullis, f. Faloona, s. Scharf, r. Saiki, g. Horn, and h. Erlich, "specific enzymatic amplification of dna in vitro: the polymerase chain reaction," cold spring harb symp quant biol, vol. 51 pt 1, pp. 263–273, 1986, doi: 10.1101/sqb.1986.051.01.032.

[24] m. Karlikow and k. Pardee, "the many roads to an ideal paper-based device," in paper-based diagnostics: current status and future applications, k. J. Land, ed. Cham: springer international publishing, 2019, pp. 171–201. Doi: 10.1007/978-3-319-96870-4_6.

[25] p. Habibzadeh, m. Mofatteh, m. Silawi, s. Ghavami, and m. A. Faghihi, “molecular diagnostic assays for covid-19: an overview,” crit rev clin lab sci, vol. 58, no. 6, pp. 385–398, sep. 2021, doi: 10.1080/10408363.2021.1884640.

[26] a. Cassedy, a. Parle-mcdermott, and r. O’kennedy, “virus detection: a review of the current and emerging molecular and immunological methods,” front mol biosci, vol. 8, p. 637559, 2021, doi: 10.3389/fmolb.2021.637559.

[27] t. Notomi et al., “loop-mediated isothermal amplification of dna,” nucleic acids res, vol. 28, no. 12, p. E63, jun. 2000, doi: 10.1093/nar/28.12.e63.

[28] m. Soroka, b. Wasowicz, and a. Rymaszewska, “loop-mediated isothermal amplification (lamp): the better sibling of pcr?,” cells, vol. 10, no. 8, p. 1931, jul. 2021, doi: 10.3390/cells10081931.

[29] “human dna polymerase η has reverse transcriptase activity in cellular environments - journal of biological chemistry.” Https://www.jbc.org/article/s0021-9258(20)36678-3/fulltext (accessed nov. 02, 2022).

[30] m. R. A. Torkaman, k. Kamachi, v. S. Nikbin, m. N. Lotfi, and f. Shahcheraghi, “comparison of loop-mediated isothermal amplification and real-time pcr for detecting bordetella pertussis,” journal of medical microbiology, vol. 64, no. 4, pp. 463–465, apr. 2015, doi: 10.1099/jmm.0.000021.

[31] “isothermal amplification of nucleic acids | chemical reviews.” Https://pubs.acs.org/doi/abs/10.1021/acs.chemrev.5b00428 (accessed nov. 02, 2022).

[32] “loop-mediated isothermal amplification | neb.” Https://www.neb.com/applications/dna-amplification-pcr-and-qpcr/isothermal-amplification/loop-mediated-isothermal-amplification-lamp (accessed nov. 11, 2022).

[33] m. K. Haleyur giri setty and i. K. Hewlett, “point of care technologies for hiv,” aids research and treatment, vol. 2014, pp. 1–20, 2014, doi: 10.1155/2014/497046.

[34] m. Murtagh and t. Peter, “art 2.0: implications for diagnostics in resource-limited settings.,” clinton health access initiative, 2010.

[35] “what is the window period for an hiv test? | guides | hiv i-base.” Https://i-base.info/guides/testing/what-is-the-window-period (accessed nov. 03, 2022).

[36] “understanding the hiv window period | testing | hiv basics | hiv/aids | cdc,” jun. 22, 2022. Https://www.cdc.gov/hiv/basics/hiv-testing/hiv-window-period.html (accessed nov. 03, 2022).

[37] a. Bangalee, s. Bhoora, and r. Punchoo, “evaluation of serological assays for the diagnosis of hiv infection in adults,” s afr fam pract (2004), vol. 63, no. 1, p. 5316, oct. 2021, doi: 10.4102/safp. V63i1.5316.

[38] g. C. Mak et al., “evaluation of rapid antigen test for detection of sars-cov-2 virus,” j clin virol, vol. 129, p. 104500, aug. 2020, doi: 10.1016/j.jcv.2020.104500.

[39] j. Fox, h. Dunn, and s. O’shea, “low rates of p24 antigen detection using a fourth-generation point of care hiv test,” sex transm infect, vol. 87, no. 2, pp. 178–179, mar. 2011, doi: 10.1136/sti.2010.042564.

[40] “advantages and disadvantages of fda-approved hiv assays used for screening,” p. 7.

[41] m. L. Schito, m. P. D’souza, s. M. Owen, and m. P. Busch, “challenges for rapid molecular hiv diagnostics,” j infect dis, vol. 201, no. Suppl 1, pp. S1–s6, apr. 2010, doi: 10.1086/650394.

[42] e. A. Phillips et al., “microfluidic rapid and autonomous analytical device (microraad) to detect hiv from whole blood samples,” lab chip, vol. 19, no. 20, pp. 3375–3386, oct. 2019, doi: 10.1039/c9lc00506d.

[43] c. S. H. Gov d. Last updated: october 25 and 2021, “global hiv/aids organizations,” hiv.gov, oct. 25, 2021. Https://www.hiv.gov/federal-response/pepfar-global-aids/global-hiv-aids-organizations (accessed may 30, 2022).

[44] j. Stone et al., “incarceration history and risk of hiv and hepatitis c virus acquisition among people who inject drugs: a systematic review and meta-analysis,” the lancet infectious diseases, vol. 18, no. 12, pp. 1397–1409, dec. 2018, doi: 10.1016/s1473-3099(18)30469-9.

[45] s. D. Wharam et al., “specific detection of dna and rna targets using a novel isothermal nucleic acid amplification assay based on the formation of a three-way junction structure,” nucleic acids res, vol. 29, no. 11, p. E54, jun. 2001.

[46] r. A. Pollini, e. Blanco, c. Crump, and m. L. Zúñiga, “a community-based study of barriers to hiv care initiation,” aids patient care stds, vol. 25, no. 10, pp. 601–609, oct. 2011, doi: 10.1089/apc.2010.0390.

[47] “global statistics,” hiv.gov. Https://www.hiv.gov/hiv-basics/overview/data-and-trends/global-statistics (accessed oct. 11, 2022).

[48] “people who inject drugs.” Https://www.who.int/teams/global-hiv-hepatitis-and-stis-programmes/populations/people-who-inject-drugs (accessed nov. 14, 2022).

[49] “world drug report 2020,” united nations: world drug report 2020. //wdr.unodc.org/wdr2020/en/index2020.html (accessed nov. 14, 2022).

[50] “basic statistics | hiv basics | hiv/aids | cdc,” jun. 21, 2022. Https://www.cdc.gov/hiv/basics/statistics.html (accessed sep. 26, 2022).

[51] “what is p24 antigen,” aidsmap.com. Https://www.aidsmap.com/about-hiv/faq/what-p24-antigen (accessed sep. 26, 2022).

[52] e. W. Fiebig et al., “dynamics of hiv viremia and antibody seroconversion in plasma donors: implications for diagnosis and staging of primary hiv infection,” aids, vol. 17, no. 13, pp. 1871–1879, sep. 2003, doi: 10.1097/00002030-200309050-00005.

[53] “stages of hiv infection,” canfar, aug. 08, 2016. Https://canfar.com/stages-of-hiv-infection/ (accessed nov. 13, 2022).

[54] “hiv care continuum | targethiv.” Https://targethiv.org/library/topics/hiv-continuum (accessed nov. 13, 2022).

[55] v. Kamat and a. Rafique, “designing binding kinetic assay on the bio-layer interferometry (bli) biosensor to characterize antibody-antigen interactions,” analytical biochemistry, vol. 536, pp. 16–31, nov. 2017, doi: 10.1016/j.ab.2017.08.002.

[56] “characterization of antibody-antigen interactions using biolayer interferometry: star protocols.” Https://star-protocols.cell.com/protocols/1008 (accessed sep. 27, 2022).

[57] “cmi_octetred384_getting_started_and_standard_protocol.pdf.” Accessed: nov. 14, 2022. [online]. Available: https://cmi.hms.harvard.edu/files/cmi/files/cmi_octetred384_getting_started_and_standard_protocol.pdf

[58] “octet-red384-system.pdf.” Accessed: nov. 13, 2022. [online]. Available: https://www.alfatestbio.it/keyportal/uploads/octet-red384-system.pdf

[59] “biosensor-selection-guide.pdf.” Accessed: nov. 13, 2022. [online]. Available: https://facilities.bioc.cam.ac.uk/files/media/biosensor-selection-guide.pdf

[60] “anti-penta-his-biosensors-for-label-free-analysis-of-his-tagged-proteins-technical-note-en-sartorius-data.pdf.” Accessed: nov. 14, 2022. [online]. Available: https://www.sartorius.com/download/552186/anti-penta-his-biosensors-for-label-free-analysis-of-his-tagged-proteins-technical-note-en-sartorius-data.pdf

[61] r. Tobias, “biomolecular binding kinetics assays on the octet platform,” p. 22.

[62] s. Kumaraswamy and r. Tobias, “label-free kinetic analysis of an antibody-antigen interaction using biolayer interferometry,” methods mol biol, vol. 1278, pp. 165–182, 2015, doi: 10.1007/978-1-4939-2425-7_10.

[63] d. Apiyo, “biomolecular binding kinetics assays on the octet® platform,” p. 28.

[64] “the need for routine viral load testing,” p. 12.

[65] “hiv.” Https://www.who.int/news-room/fact-sheets/detail/hiv-aids (accessed nov. 15, 2022).

[66] f. M. Hecht et al., “hiv rna level in early infection is predicted by viral load in the transmission source,” aids, vol. 24, no. 7, pp. 941–945, apr. 2010, doi: 10.1097/qad.0b013e328337b12e.

[67] e. A. Ochodo, e. E. Olwanda, j. J. Deeks, and s. Mallett, “point-of-care viral load tests to detect high hiv viral load in people living with hiv/aids attending health facilities,” cochrane database syst rev, vol. 2022, no. 3, p. Cd013208, mar. 2022, doi: 10.1002/14651858.cd013208.pub2.

[68] k. N. Clayton, g. D. Berglund, j. C. Linnes, t. L. Kinzer-ursem, and s. T. Wereley, “dna microviscosity characterization with particle diffusometry for downstream dna detection applications,” anal. Chem., vol. 89, no. 24, pp. 13334–13341, dec. 2017, doi: 10.1021/acs.analchem.7b03513.

[69] k. N. Clayton, t. J. Moehling, d. H. Lee, s. T. Wereley, j. C. Linnes, and t. L. Kinzer-ursem, “particle diffusometry: an optical detection method for vibrio cholerae presence in environmental water samples,” sci rep, vol. 9, no. 1, art. No. 1, feb. 2019, doi: 10.1038/s41598-018-38056-7.

[70] oneblood and solodev, “the science behind separating blood and platelets | oneblood,” aug. 05, 2019. Https://www.oneblood.org/media/blog/platelets/the-science-behind-separating-blood-and-platelets.stml (accessed nov. 16, 2022).

[71] a. J. Colbert, d. H. Lee, k. N. Clayton, s. T. Wereley, j. C. Linnes, and t. L. Kinzer-ursem, “pd-lamp smartphone detection of sars-cov-2 on chip,” anal chim acta, vol. 1203, p. 339702, apr. 2022, doi: 10.1016/j.aca.2022.339702.

[72] a. A. Waheed and e. O. Freed, “hiv type 1 gag as a target for antiviral therapy,” aids res hum retroviruses, vol. 28, no. 1, pp. 54–75, jan. 2012, doi: 10.1089/aid.2011.0230.

[73] r. Craigie, “the molecular biology of hiv integrase,” future virol, vol. 7, no. 7, pp. 679–686, jul. 2012, doi: 10.2217/fvl.12.56.

[74] “integrase | nih.” Https://clinicalinfo.hiv.gov/en/glossary/integrase (accessed oct. 12, 2022).

[75] “optigene-lamp-user-guide-assay-design-primers-1.pdf.” Accessed: nov. 15, 2022. [online]. Available: http://www.optigene.co.uk/wp-content/uploads/2012/06/optigene-lamp-user-guide-assay-design-primers-1.pdf

[76] “bst dna polymerase | meridian bioscience | meridian bioscience.” Https://www.meridianbioscience.com/lifescience/products/molecular-reagents/dna-polymerases/bst-dna-polymerase/ (accessed oct. 19, 2022).

[77] d. Lee, y. Shin, s. Chung, k. S. Hwang, d. S. Yoon, and j. H. Lee, “simple and highly sensitive molecular diagnosis of zika virus by lateral flow assays,” anal. Chem., vol. 88, no. 24, pp. 12272–12278, dec. 2016, doi: 10.1021/acs.analchem.6b03460.

[78] n. A. Tanner, y. Zhang, and t. C. Evans, “simultaneous multiple target detection in real-time loop-mediated isothermal amplification,” biotechniques, vol. 53, no. 2, pp. 81–89, aug. 2012, doi: 10.2144/0000113902.

[79] s. Bhadra, y. S. Jiang, m. R. Kumar, r. F. Johnson, l. E. Hensley, and a. D. Ellington, “real-time sequence-validated loop-mediated isothermal amplification assays for detection of middle east respiratory syndrome coronavirus (mers-cov),” plos one, vol. 10, no. 4, p. E0123126, apr. 2015, doi: 10.1371/journal.pone.0123126.

[80] “warmstart® lamp kit (dna & rna) | neb.” Https://www.neb.com/products/e1700-warmstart-lamp-kit-dna-rna#product%20information (accessed oct. 19, 2022).

[81] s. Kemleu et al., “a field-tailored reverse transcription loop-mediated isothermal assay for high sensitivity detection of plasmodium falciparum infections,” plos one, vol. 11, no. 11, p. E0165506, 2016, doi: 10.1371/journal.pone.0165506.

[82] “halt^{tm} protease inhibitor cocktail (100x).” Https://www.thermofisher.com/order/catalog/product/78430 (accessed oct. 19, 2022).

[83] “ebioscience^{tm} 1x rbc lysis buffer.” Https://www.thermofisher.com/order/catalog/product/00-4333-57 (accessed nov. 17, 2022).

[84] m. Black, “rbc lysing solutions and cell lysing procedure,” p. 1.